Title
Charged-Particle Irradiation of Intracranial Lesions

Authors
Levy, R.P.
Fabrikant, J.I.
Steinberg, G.K.
et al.

Publication Date
1993

LBL-33797
UC-408

Lawrence Berkeley Laboratory
UNIVERSITY OF CALIFORNIA

To be published as a chapter in *Neurosurgery*,
R.H. Wilkins, and S.S. Rengachary, Eds.,
McGraw-Hill, New York, NY, June 1993

Charged-Particle Irradiation of Intracranial Lesions

R.P. Levy, J.I. Fabrikant, G.K. Steinberg, and K.A. Frankel

March 1993

Donner Laboratory

Biology & Medicine Division

Prepared for the U.S. Department of Energy under Contract Number DE-AC03-76SF00098

DISCLAIMER

LBL-33797

Charged-Particle Irradiation of Intracranial Lesions

In **R. H. Wilkins, S. S. Rengachary (eds):**
NEUROSURGERY
McGraw-Hill, New York, 1994

Richard P. Levy, M.D., Ph.D.

Jacob I. Fabrikant, M.D., Ph.D.

Gary K. Steinberg, M.D., Ph.D.

Kenneth A. Frankel, Ph.D.

Life Sciences Division
Lawrence Berkeley Laboratory
University of California at Berkeley
Berkeley, CA 94720

March 1993

This research was supported by the Director, Office of Energy Research, Office of Health and Environmental Research, Medical Applications Division of the U.S. Department of Energy under Contract No. DE-AC03-76SF00098.

CHARGED-PARTICLE IRRADIATION OF INTRACRANIAL LESIONS[1]

Richard P. Levy, M.D., Ph.D.,[†] Jacob I. Fabrikant, M.D., Ph.D.,[‡] Gary K. Steinberg, M.D., Ph.D., [§] Kenneth A. Frankel, Ph.D.[‖]

[†] Assistant Adjunct Professor of Radiology, University of California, San Francisco; Medical Scientist and Staff Scientist, Donner Pavilion and Donner Laboratory, Division of Life Sciences, Lawrence Berkeley Laboratory, University of California, Berkeley, California

[‡] Professor of Radiology, University of California, San Francisco and Berkeley; Medical Scientist and Senior Scientist, Donner Pavilion and Donner Laboratory, Division of Life Sciences, Lawrence Berkeley Laboratory, University of California, Berkeley, California

[§] Associate Professor of Neurosurgery, Stanford University School of Medicine, Stanford, California

[‖] Assistant Adjunct Professor of Radiology, University of California, San Francisco; Staff Scientist, Donner Pavilion and Donner Laboratory, Division of Life Sciences, Lawrence Berkeley Laboratory, University of California, Berkeley, California

Direct correspondence to:

Richard P. Levy, M.D., Ph.D.
Donner Pavilion and Donner Laboratory
University of California at Berkeley
Berkeley, California 94720
Telephone: (510) 486-7479

[1]Research supported by the Director, Office of Energy, Health and Environmental Research of the United States Department of Energy under Contract DE-AC03-76SF00098.

INTRODUCTION

Charged-particle irradiation of intracranial lesions has been the subject of biomedical research and clinical development since 1946, when Wilson [76] proposed the therapeutic use of charged-particle beams, based on the unique physical characteristics of alpha-emitting radionuclides first observed by Bragg in 1904 [4]. After completion of the 184-inch synchrocyclotron at the University of California at Berkeley - Lawrence Berkeley Laboratory (UCB-LBL) in 1947 [5], Tobias and Lawrence and their colleagues [72,73,74] began the study of the biologic effects of beams of protons, deuterons and helium ions, with particular emphasis on reaction to radiation injury in the brain.

Since 1954, more than 7,000 patients world-wide with intracranial and juxtaspinal lesions have been treated with charged-particle irradiation[1]. The majority of these patients have been treated at UCB-LBL [7,16,38,66], the Harvard Cyclotron Laboratory - Massachusetts General Hospital (HCL-MGH) [24,25,27,69], the Institute for Theoretical and Experimental Physics in Moscow (ITEP) [58,61] and the Institute of Nuclear Physics in St. Petersburg (INPh) [28]. Most patients have been treated with single-dose irradiation or with a few large-dose fractions (i.e., a *stereotactic radiosurgical* approach), but several hundred patients with primary malignant tumors have been treated using conventional fractionation schedules [6,7,8,69].

Clinical applications were constrained initially by the limitations of neuroradiologic techniques for treatment planning, stereotactic localization and dose distribution [38]. Early clinical trials, therefore, were restricted to pituitary-ablation treatment, in which high-dose radiation was used to induce selective destruction of small, well-defined intracranial target volumes. The first stereotactic irradiation procedures utilizing charged particles in clinical patients were performed by Lawrence and colleagues [31] at UCB-LBL in 1954 for pituitary-hormone suppression in the treatment of metastatic breast carcinoma. Shortly thereafter, charged-particle radiosurgery was applied to the pituitary-ablation treatment of patients

[1]Only charged particles of proton mass or greater are considered in this chapter.

with proliferative diabetic retinopathy [34,36] and to the treatment of pituitary adenomas [27,35,45]. During these early years, limited numbers of patients were also treated for other conditions, including certain functional disorders and malignant brain tumors [35]. With the development of improved techniques of stereotaxis and cerebral angiography, the charged-particle radiosurgical approach, using Bragg-peak protons, was applied to the treatment of arteriovenous malformations (AVMs) at HCL-MGH by Kjellberg et al [24] in 1965. More recently, the advent of high-resolution computed X-ray tomography (CT) and magnetic resonance imaging (MRI) has made it possible for reliable stereotactic localization and irradiation techniques to be applied to the treatment of a diverse collection of disorders [37]. The expanded application of charged-particle irradiation for intracranial lesions is an important development in neurosurgery and radiation oncology, which promises new and innovative approaches that will influence therapeutic strategies, not only in the brain but elsewhere in the central nervous system and at other sites within the body. In the past few years, advances in neurologic imaging have been accompanied by technological advances and by computer software dedicated to charged-particle treatment planning and dose delivery. During the past five years, especially, all these factors have contributed to increased numbers of institutions world-wide building and/or planning charged-particle treatment facilities [38].

The objectives of this chapter are to present the rationale for the use of charged-particle irradiation as a neurosurgical and/or radiotherapeutic procedure and to describe the spectrum of human research studies thus far carried out in the development of charged-particle irradiation for intracranial lesions. A comprehensive review of these topics is beyond the scope of this chapter. Selected historically significant or representative studies and reviews, therefore, have been summarized and/or cited for further reference.

PHYSICAL PROPERTIES OF CHARGED-PARTICLE BEAMS

Ionizing radiations used for external-beam irradiation may be classified as high-energy photons (e.g., X-rays or gamma rays) or accelerated charged particles (e.g., protons or helium ions). As photons traverse and interact with tissue, their ionization events attenuate with depth in tissue (Fig. 1); satisfactory dose distributions in deep-seated lesions are achieved, at the cost of a relatively high integral dose to the patient, by using beams from many different angles or intersecting dynamic arcs. Charged-particle beams manifest very different physical properties that can be exploited to place a high dose of radiation preferentially within the boundaries of a deeply located target volume [19,38,63]. These properties include: (1) a well-defined *range* that can be adjusted precisely so that the beam *stops* at the distal edge of the target and deep within the tissue, resulting in little or no exit dose; (2) an initial region of low dose (the *plateau*) as the beam penetrates through tissue, followed by a region of high dose (the *Bragg ionization peak*) at the end of the range of the beam which can be adjusted to conform to the location and dimensions of the target, so that the entrance dose can be kept to a minimum; and (3) very sharp lateral edges that can be shaped by metal apertures to conform to the projected cross-sectional contour of the target, so that negligible dose is absorbed by the adjacent normal tissues (Figs. 1, 2, 3, 4).

Each charged-particle beam can be directed to place individually shaped three-dimensional high-dose regions precisely within the brain by using an appropriately shaped aperture, spreading the Bragg peak and adjusting the beam range (Fig. 3). For irregularly shaped lesions and to accommodate skull curvature, tissue-equivalent compensators positioned in the beam path are used to match the distal edge of the spread-out Bragg peak (across the transverse profile of the beam) to the distal surface of the target volume [19,38]. Several entry angles and beam ports (typically, four) are directed stereotactically so that the high-dose regions of the individual beams intersect within the target volume, with a much lower dose to immediately adjacent and intervening normal brain tissues [16,19,38,39].

TREATMENT PLANNING AND DOSE DELIVERY[2]

[2]Portions of this section are adapted with permission from: KA Frankel [19].

The application of charged-particle irradiation to the treatment of intracranial lesions presents a number of problems not encountered in conventional radiotherapy [10,19,75]. Treatment planning and dose delivery consist of sequential neuroradiologic imaging studies, computer-assisted image correlation and calculation of dose distribution, positioning of the patient and target volume within a three-dimensional frame of reference, and delivery to the target of carefully monitored charged-particle beams [16,19,53,64]. In this section, we consider briefly the methods of treatment planning and dose delivery that have been developed at UCB-LBL for stereotactic radiosurgery for Bragg-peak and plateau-beam irradiation of vascular and other disorders; similar techniques in principle are employed at other charged-particle facilities and are applicable as well to extended-fractionation delivery of charged-particle irradiation. The reader is referred to Frankel et al [19] for a more-detailed review.

STEREOTACTIC LOCALIZATION

A transportable stereotactic frame-mask system, consisting of an individualized thermoplastic immobilizing head mask and stereotactic frame with fiducial markers, has been developed to permit accurate and reproducible positioning of the patient's head for neuroradiologic procedures, including target definition and localization, treatment planning and radiosurgical treatment (Fig. 5) [53]. The stereotactic frame can be attached to neuroradiologic couches and to the stereotactic positioning couch – the Irradiation Stereotactic Apparatus for Humans (ISAH) (Fig. 4) [52,53]. This system has proven to be safe and reliable in more than 1,300 patients [38].

NEURORADIOLOGIC EVALUATION AND IMAGE CORRELATION

Methods for correlation of stereotactic MRI and CT images have been developed for target definition and localization for neoplastic disorders and angiographically occult vascular malformations (AOVMs) [16,19,42]. In the patient whose brain-stem lesion is illustrated in Fig. 6, radiosurgical target contours are delineated on stereotactic MRI and CT images.

The MRI-derived target contours are transferred to CT for comparison with CT-derived contours, and a final set of target contours is then defined on the noncontrast CT images. For each CT slice, the inner and outer tables of the skull are digitized, along with selected other bony landmarks, such as the pituitary sella, frontal plates and anterior and posterior protuberances. A computerized digitization program then generates CT-derived treatment-localization overlays (alignment aids), based on the final target contours and the digitized bony landmarks [64]. The CT data are also used to determine the coordinates required to position the patient on ISAH. The radiosurgical treatment of pituitary adenomas represents a special situation for which the localization procedure is greatly simplified, because the sella turcica can usually be readily identified and localized on plain orthogonal radiographs [19].

For AVMs, stereotactic cerebral angiography is the most precise imaging method for determining the shape and location of the lesion. (MRI and CT imaging, however, are useful for demonstrating relationships of the AVM to adjacent anatomic structures.) The contours of the AVM target, derived from selected orthogonal angiographic films and transferred to the CT images, form the basis for the stereotactic treatment-planning procedure [16, 19,64]. Via geometric optics, the digitization program uses the positions of the fiducial markers of the stereotactic frame as they appear on the radiographs, in conjunction with their known positions on the frame, to calculate radiographic magnification factors and the coordinates of the target volume within the frame. The digitized angiographic data are also used to calculate the initial translational coordinates of the patient-positioning couch and to generate overlays of the stereotactic-frame fiducial markers, angiographically derived target contours and midplane bony landmarks of the skull for lateral and anteroposterior localization radiographs (Fig. 7).

The digitization program also models the angiographically derived AVM target volume as a series of ellipses on corresponding axial CT slices. The CT data and derived target contours for each axial CT slice are reformatted to generate relevant views in coronal and sagittal planes. The reformatted target contours, which are corrected for parallax and magnification, then have approximately the same shape and location as the AVM target delineated on the orthogonal angiographic films [64]. In the case of irregularly shaped AVMs, MRI and CT image information may be used to modify the target contours [19].

COMPUTER-ASSISTED TREATMENT PLANNING

For homogeneous tissues, the task of positioning the Bragg peak at a specified depth is quite straightforward. For the heterogeneous tissues of the skull and brain, however, this procedure is more complex [10,75]. Generally, denser bone tissue slows the incident stream of charged particles more per unit length of tissue than does less dense parenchymal tissue. Thus, a beam traversing denser tissue will have its Bragg-peak region displaced proximally to a greater extent than a beam traversing less dense tissue. Knowledge of the physical characteristics of each volume element of tissue along the beam path on a pixel-by-pixel basis is necessary for precise determination of dose distribution and for calculating the depth of penetration of the beam. Noncontrast-CT data provide electron-density information (X-ray absorption coefficients), which is converted to charged-particle energy loss by established calibration functions [10]. Dose-absorbing filters of appropriate thickness are placed in the beam path to adjust the range in tissue precisely to the desired value (Fig. 4).

A computer-assisted treatment-planning program is used to calculate dose distributions and to generate isodose curves [10]. Figures 8 and 9 are representative examples of the isodose-contour displays of treatment plans for small and large AVMs, respectively. The size, shape and location of the lesion, and the dose to the target volume and adjacent brain structures are interrelated factors that affect the choice of beam ports, entry angles and dose-configuration patterns. The final treatment plan is selected after iterative refinement of a number of preliminary treatment plans.

TARGET LOCALIZATION AND TREATMENT PROCEDURE

The radiosurgical procedure requires that the target volume be localized precisely at the intersection of the charged-particle beam and the isocenter of ISAH [52]. ISAH has three degrees of freedom for translation, two degrees of freedom for rotation (the third degree of rotational freedom is effected by rotation of the beam-shaping aperture) and a mechanical precision of 0.1 mm and 0.1°. (Based upon the limits of resolution of imaging data and correlation and the intrinsic uncertainties in patient positioning, the overall localization and alignment system is reproducible in repeated diagnostic and therapeutic sessions to approximately 1.5 mm and 1.5° in each translational and rotational degree of freedom, respectively [53,64].)

At treatment, the patient is positioned on ISAH in the stereotactic frame-mask system, and orthogonal localization radiographs are performed. Final alignment of the patient is verified by comparing the localization radiographs and port films exposed immediately prior to treatment to the computer-generated treatment-localization overlays [16,19]. The treatment beams are delivered through a number of beam ports by rotating the patient's head and/or treatment couch sequentially to predetermined fixed positions. Each beam port requires 10 to 15 minutes for patient positioning, aperture adjustment and compensator placement and 1 to 3 minutes for beam exposure. The entire treatment procedure typically requires about 30 to 60 minutes.

PLATEAU-BEAM STEREOTACTIC IRRADIATION

When a charged-particle beam of sufficiently high energy, and hence greater depth of penetration, is available, radiosurgery can be performed with the plateau-ionization portion of the beam. In this treatment configuration, the beam passes completely through the head, depositing plateau-region radiation in the brain; the Bragg-peak dose is absorbed in the wall of the the treatment room opposite the beam line. This method was developed by Lawrence and colleagues [30,31,70,73] at UCB-LBL for irradiation of the pituitary gland with plateau beams of protons and (subsequently) helium ions, and it is currently applied to radiosurgery of small intracranial target volumes at several proton-irradiation centers in Russia [28,60,61].

With the plateau-beam-irradiation technique, consideration of the tissue inhomogeneity normally encountered in the head is not important, but accurate stereotactic localization of the intracranial target volume and precise isocentric technique are essential. The plateau-beam radiosurgical system developed at UCB-LBL uses a stereotactic positioning table and head holder in combination with individually fabricated plastic head masks for immobilization (Fig. 10). Following delineation of the target volume, the charged-particle beam is centered on the sella turcica by means of orthogonal localization radiographs and port films, and the beam contour is shaped by a brass aperture. During irradiation, the head is turned in pendulum motion around a horizontal axis while the patient is positioned sequentially at 12 discrete angles around a vertical axis (Fig. 10). The irradiation arcs are directed such that the dose fall-off is very rapid in the anteroposterior direction and toward the optic chiasm; the dose fall-off decreases more slowly laterally toward the temporal lobes (Fig. 11). With this method, the optic chiasm, hypothalamus and outer portions of the sphenoid sinus receive less than 10% of the central-axis pituitary dose [70]. Plateau-beam radiosurgery can also be used for treatment of disorders other than pituitary adenomas. For these applications, however, it is necessary to incorporate the more-general methods of stereotactic target localization described previously [19].

The dose distributions that result from the use of isocentrically directed arcs of plateau-beam irradiation are quite comparable to those produced with stereotactic radiosurgical systems using X-rays or gamma rays. Their application, therefore, is similarly limited primarily to the treatment of lesions less than 2 to 3-cm diameter [63].

CLINICAL APPLICATIONS[3]

Four decades have now passed since the first patient was treated with charged-particle irradiation of the brain. Clinical experience has been obtained in the following categories: pituitary hormone suppression, pituitary adenomas, malignant gliomas, vascular malformations, juxtaspinal tumors and ocular melanomas. In this section, we review selected aspects

[3]Portions of this section are adapted with permission from: JI Fabrikant [16], RP Levy [38], and GK Steinberg [66,68].

of the world-wide clinical experience with charged-particle irradiation of intracranial and juxtaspinal lesions; for more-detailed information, the reader is referred to several recent reviews [14,16,37,38]. The relative emphasis here on helium-ion irradiation reflects the authors' experience at UCB-LBL and at Stanford University Medical Center (SUMC); this experience has been paralleled by extensive experience with proton-beam therapy elsewhere.

PITUITARY HORMONE SUPPRESSION

Charged-particle irradiation of the pituitary gland has been shown in more than 1,300 patients to be very effective for inducing suppression of normal pituitary function with minimal associated risk of inducing injury in adjacent neural structures [38,65]. The primary applications of charged-particle hypophysectomy have been to control the metastatic spread of selected hormone-responsive carcinomas (e.g., breast and prostate cancer) [11,28,31,32, 34,35,48,58,61,62,73] and to induce regression of proliferative diabetic retinopathy [26,28, 34,36,44,58,61].

In North America, pituitary-ablation treatment is no longer in common use. In the case of metastatic breast carcinoma, for example, modern anti-estrogenic drugs are now available for selective use, guided, in part, by reliable estrogen-receptor classification of tumors. In the case of diabetic retinopathy, pituitary-ablation treatment has also fallen out of favor. Nonetheless, the extensive clinical experience accrued has served to provide considerable information about radiation tolerance of the pituitary gland, parasellar tissues, cranial nerves and temporal lobes [65].

Hormone-Dependent Metastatic Carcinoma

Between 1954 and 1972 at UCB-LBL, stereotactically directed plateau beams of protons (initial 26 cases) or helium ions (157 cases) were used for pituitary-ablation treatment in 183 patients with metastatic breast carcinoma [35]. Patients received 180 to 220 Gy stereotactic plateau-beam helium-ion irradiation to the pituitary gland, in order to control the metastatic spread of carcinoma by effecting hormonal suppression through induction of hypopituitarism. The total dose was given in six to eight fractions over 2 to 3 weeks in the early years of the clinical program and in three or four fractions over 5 days in later years. Each dose fraction consisted of 30 to 50 Gy. Many patients experienced long-term remissions. Eight cases of focal radiation necrosis limited to the adjacent portion of the temporal lobe occurred; all were from an earlier group of patients who had received higher doses to suppress pituitary function as rapidly as possible [56]. Clinical manifestations of temporal lobe injury and transient cranial nerve involvement occurred in only four of these patients.

Minakova et al [48,62] have reported excellent results following stereotactic plateau-beam proton radiosurgery at ITEP in a series of 489 patients with metastatic breast carcinoma and in a series of 92 patients with metastatic prostate carcinoma (Ye. I. Minakova, personal communication). Konnov et al [28] have also reported excellent clinical results in breast carcinoma patients treated with 120 to 180 Gy plateau-beam proton radiosurgery at INPh. In a series of 91 patients with bone metastases, 93% had relief of pain following treatment. Of 45 patients treated for metastatic disease with combined medical therapy and proton-beam hypophysectomy, 20 had no signs of recurrence or metastases after a follow-up period of 2 to 6 years. Kjellberg et al have used Bragg-peak proton-beam therapy of the pituitary to treat 31 patients with metastatic breast cancer at HCL-MGH (R. N. Kjellberg, personal communication).

Diabetic Retinopathy

Between 1958 and 1969 at UCB-LBL, 169 patients with proliferative diabetic retinopathy received stereotactic plateau-beam helium-ion pituitary irradiation. This procedure was performed to evaluate the effects of pituitary hormonal suppression on proliferative diabetic retinopathy. (Earlier reports had suggested that surgical hypophysectomy resulted in regression of proliferative retinopathy in many diabetic patients, a phenomenon suspected to be related to decreased insulin requirements and lowered growth hormone (GH) levels

[50].) The first 30 patients in this cohort were treated with 160 to 320 Gy delivered in six to eight fractions (27 to 50 Gy per fraction) over 11 days to effect total pituitary ablation; the subsequent 139 patients underwent subtotal pituitary ablation with 80 to 150 Gy. Most patients had a 15 to 50% decrease in insulin requirements; this result occurred sooner in patients receiving higher doses, but ultimately both patient groups had comparable insulin requirements. Fasting GH levels and reserves were lowered within several months after irradiation. Moderate to good vision was preserved in at least one eye in 59 of 114 patients at 5 years after pituitary irradiation (J.H. Lawrence, unpublished). Of 169 patients treated, 69 patients (41%) ultimately required thyroid replacement and 46 patients (27%) required adrenal hormone replacement. There were four deaths from complications of hypopituitarism. Focal temporal lobe injury was limited to an early group of patients that had received at least 230 Gy to effect rapid pituitary ablation in advanced disease; four patients in this high-dose group developed extraocular palsies. Neurologic injury was rare in those patients receiving doses less than 230 Gy (J.H. Lawrence, unpublished).

In a series of 25 patients treated with 100 to 120 Gy plateau-beam proton radiosurgery, Konnov et al [28] found that those with higher visual acuity and without proliferative changes in the fundus had stabilization and regression of retinopathy after treatment; microaneurysms were decreased and visual acuity was stabilized or improved. However, patients with poor visual acuity and progressive proliferative retinopathy responded less favorably. A reduction in insulin requirements was observed in all patients. Kjellberg et al [26] reported comparable results following stereotactic Bragg-peak proton radiosurgery in 183 patients.

Histopathologic Studies

Histopathologic observations on autopsies from early patients, who had received helium-ion pituitary irradiation for hormonal suppression of metastatic breast carcinoma, confirmed that more than 95% of pituitary cells were destroyed and replaced with connective tissue in a period of several months with doses of 180 to 220 Gy delivered in 2 or 3 weeks total time (Fig. 12) [56,77]. At lower doses, the magnitude of the histologic effect depended on the dose at the periphery of the pituitary gland, where viable hormone-secreting cells were usually found.

Woodruff et al [77] performed autopsies on 15 patients who had been treated with stereotactic plateau-beam helium-ion irradiation of the pituitary gland at UCB-LBL. Ten of these patients had been treated for progressive diabetic retinopathy with average doses of 116 Gy delivered in six fractions. All cases demonstrated pituitary fibrosis without radiation changes in the surrounding brain tissue or cranial nerves.

PITUITARY ADENOMAS

Since 1958, more than 2,000 patients world-wide with pituitary adenomas have been treated with charged-particle irradiation of the pituitary gland as a primary noninvasive treatment, as adjunctive radiation therapy for incomplete operative resection and/or medical therapy and as treatment for late recurrences after surgery [25,27,28,33,43,45,51,60]. Charged-particle radiosurgery has been applied to the treatment of acromegaly, Cushing's disease, Nelson's syndrome and prolactin-secreting tumors, as well as to the treatment of nonfunctioning and selected other adenomas.

Prior to the introduction of transsphenoidal microsurgery, surgical hypophysectomy was often associated with high morbidity and mortality, and charged-particle radiosurgery was considered to be an excellent alternative treatment. With the development of safe and effective transsphenoidal techniques, the extensive clinical use of primary radiosurgical treatment, concentrated for many years in the UCB-LBL and HCL-MGH programs, has decreased significantly. Currently, primary radiosurgery for treatment of microadenomas is most often limited to patients who are considered to be poor surgical candidates or who have refused surgery. Proton-beam radiosurgery, however, remains as a primary therapeutic procedure for treatment of pituitary tumors in Russia [28,38,51,59,60]. The charged-particle radiosurgical approach is now being applied mostly as adjunctive therapy in combination with microsurgery, where complete removal of large adenomas is not possible, or for recurrences of tumor growth.

The therapeutic goals in the primary radiosurgical treatment of pituitary adenomas are control of tumor growth and hormonal hypersecretion, with acceptably low hormonal and neurologic complications. These goals have been met with remarkable success over the past 35 years, especially considering the limitations of the available neuroradiologic imaging methods during the early years of these investigations. (The great majority of patients were treated before the advent of CT and MRI, and adenoma assessment and target-volume determination, therefore, relied on relatively crude neuroradiologic procedures such as polytomography and pneumoencephalography.) The clinical and metabolic follow-up data describing the response of pituitary adenomas to charged-particle radiosurgery have been reported extensively; the reader is referred to references [14] and [38] for more-detailed reviews. In this section, the emphasis is limited to selected clinical studies and complications of treatment.

Acromegaly

At UCB-LBL, stereotactic helium-ion plateau-beam radiosurgery has proven to be very effective for the treatment of acromegaly in 318 patients [30,33,43]. The maximum dose to the pituitary tumor ranged from 30 to 50 Gy, most often delivered in four fractions over 5 days. The choice of dose varied according to the extent of disease and the corresponding size of the target volume. Maximum pituitary doses were selected so that the cortex of the temporal lobes received no more than 15 Gy. As the dose fell off rapidly from the central axis, the dose to the periphery of larger tumors was considerably less than the peripheral dose to smaller ones. A sustained decrease in serum-GH secretion was observed in most patients; the mean serum-GH level in a cohort of 234 of these patients decreased nearly 70% within 1 year and continued to decrease thereafter (Fig. 13). Normal levels were sustained during more than 10 years of follow-up. Comparable long-term results were observed in a cohort of 65 patients who were irradiated with helium ions because of residual or recurrent metabolic abnormalities persisting after surgical hypophysectomy. Serial GH levels were examined before and after helium-ion irradiation as a function of neurosurgical grade. Statistically significant differences ($p < 0.01$) in fasting GH existed only between the microadenoma patients with normal sellar volumes (Hardy's Grade I [21]) and patients with macroadenomas (Grades II through IV) [43]. Grade I patients had lower initial GH levels, responded more rapidly to treatment, and had a good prognosis for cure; a lower incidence of post-treatment hypopituitarism was also observed in these patients. The more invasive tumors were slower to respond, but by 4 years after irradiation they were associated with GH levels not statistically different from levels found in patients with Grade I tumors. Clinical and metabolic improvement (e.g., improved glucose tolerance, normalization of serum phosphorus levels) was observed in most patients within the first year, even before a significant fall in serum-GH level was noted.

Treatment failures following helium-ion irradiation generally resulted from failure to assess accurately the degree of extrasellar tumor extension [33,43]. With recent advances in MRI and CT scanning, the radiosurgical target can now be better delineated, which in turn should lead to improved rates of tumor cure and control. These same imaging improvements also make possible more reliable determination of tissue inhomogeneities in the brain and adjacent tissues and correspondingly more precise positioning of the Bragg ionization peak within the target volume [19,38].

Kjellberg et al [25,27] have treated about 600 patients with acromegaly using Bragg-peak proton irradiation at HCL-MGH. Using a nomogram based on lesion size and complication rate in a large number of treated patients, doses selected are inversely related to the beam diameter; intrasellar tumors typically receive maximal central doses of 60 to 120 Gy. Selected adenomas with extrasellar extension are treated using a "beam-within-a-beam" technique; here, a subnecrotizing dose (e.g., 10 Gy) is given to the larger overall target volume, and an additional necrotizing dose (e.g., 35 Gy) is given to the smaller intraclinoid volume. Therapy has resulted in objective clinical improvement in about 90% of a cohort of 145 patients 24 months after irradiation. By this time, 60% of patients were in remission (GH level $\leq$ 10 ng/mL); after 48 months, 80% were in remission. About 10% of patients failed to enter remission or to improve, and they required additional treatment (usually transsphenoidal hypophysectomy).

Another approach under consideration for the charged-particle-irradiation treatment of invasive macroadenomas is the use of more extended fractionation schedules. Historically, stereotactic irradiation regimens have not been designed to exploit the differential response between normal cells and tumor cells that is the biologic basis for the use of fractionated external-beam irradiation [41]. With the development of stereotactic immobilization systems capable of reliable serial repositioning, this approach offers the potential for improved treatment outcome by combining the excellent dose-localization and dose-distribution characteristics of charged-particle irradiation with the favorable radiobiologic properties of fractionated irradiation.

In the Russian experience, plateau-beam proton radiosurgery has also proven successful for treatment of acromegalic tumors. Minakova et al [60] reported excellent results in 93 patients with acromegaly treated at ITEP. Konnov et al [28] observed partial or total remission in 89% of 145 patients treated with doses of 100 to 120 Gy at INPh.

Cushing's Disease

Cushing's disease has been treated successfully at UCB-LBL using stereotactic helium-ion plateau-beam irradiation [33,43,45]. In 83 patients (aged 17-78 years) treated, mean basal cortisol levels in a cohort of 44 patients and urinary fluorogenic corticosteroids in a cohort of 37 patients returned to normal values within 1 year after treatment, and these indices remained normal during more than 10 years of follow-up (Fig. 14). All five teenage patients were cured by doses of 60 to 120 Gy without concomitant hypopituitarism or neurologic sequelae; however, nine of 59 older patients subsequently underwent bilateral adrenalectomy or surgical hypophysectomy due to relapse or failure to respond to treatment. Of the nine treatment failures, seven occurred in the earlier group of 22 patients treated with 60 to 150 Gy in six alternate-day fractions; when the same total doses were given in three or four daily fractions, 40 of 42 patients were cured [43].

Kjellberg et al [25] have treated more than 175 Cushing's disease patients with Bragg-peak proton-beam irradiation at HCL-MGH. Doses are inversely related to the beam diameter selected (typically, 60 to 120 Gy). Complete remission with restoration of normal clinical and laboratory findings has occurred in about 65% of a cohort of patients followed-up for 24 months; another 20% were improved to the extent that no further treatment was considered necessary.

Minakova et al [58,60] have reported excellent results in 224 Cushing's disease patients treated with plateau-beam proton radiosurgery at ITEP. Konnov et al [28] have reported that plateau-beam proton radiosurgery (doses, 100 to 120 Gy) has induced partial or total remission in 34 of 37 patients who were followed 6 to 15 months after treatment.

Nelson's Syndrome

Plateau-beam helium-ion radiosurgery has been used at UCB-LBL in 17 patients with Nelson's syndrome [33,43]. Treatment doses and fractionation schedules were comparable to those for the Cushing's disease group, i.e., 50 to 150 Gy in four fractions. Six patients had prior pituitary surgery, but persistent tumor or elevated serum ACTH levels indicated that further treatment was required. All patients in the Nelson's syndrome group had marked decreases in ACTH levels, but rarely to normal levels. All but one patient, however, had neuroradiologic evidence of local tumor control.

Kjellberg and Kliman [25] reported similar findings in patients treated with Bragg-peak proton irradiation. Of a cohort of 19 patients treated, 12 of 14 patients experienced some depigmentation following treatment; headache was reduced or eliminated in eight of 11 patients. ACTH levels were decreased in all four patients for whom data were available, but levels became normal in only one patient.

Prolactin-Secreting Adenomas

Twenty-nine patients with prolactin-secreting pituitary tumors were treated at UCB-LBL using stereotactic plateau-beam helium-ion radiosurgery [30,43]. Treatment dose and fractionation were comparable to that in the Cushing's disease and Nelson's syndrome groups, i.e., 50 to 150 Gy in four fractions. Helium-ion irradiation was the sole treatment in 17 patients; the remaining patients were irradiated after surgical hypophysectomy had failed to provide complete or permanent improvement. Of 20 patients followed 1 year after irradiation, 19 had a marked fall in prolactin level (12 to normal levels) (Fig. 15). Amenorrhea and galactorrhea often resolved before prolactin levels returned to normal [43]. Two patients became pregnant after treatment.

Konnov et al [28] have reported partial or total remission in about 85% of patients with prolactin-secreting tumors treated with plateau-beam proton radiosurgery (doses, 100 to 120 Gy) at INPh. Excellent clinical results have also been reported in 75 patients treated with plateau-beam proton radiosurgery at ITEP (Ye. I. Minakova, personal communication), and in 132 patients treated with Bragg-peak proton therapy at HCL-MGH (R. N. Kjellberg, personal communication).

Complications

Variable degrees of hypopituitarism developed as sequelae of attempts at subtotal destruction of pituitary function in about one third of the patients following stereotactic helium-ion plateau-beam radiosurgery, although endocrine deficiencies were rapidly corrected in most cases with appropriate hormonal replacement therapy [43,65]. Retrospectively, it appears likely that, in many cases, larger portions of the pituitary gland had to be designated for radiosurgical treatment to assure sufficient dose to the adenoma than would now be indicated based on current MRI and CT techniques. Diabetes insipidus has not been observed in any pituitary patient treated with helium-ion irradiation [43]. Other than hormonal insufficiency, complications in the pituitary tumor patients treated with helium-ion plateau radiosurgery were relatively few and limited most frequently to those patients who had received prior photon irradiation. These sequelae included mild or transient extraocular nerve palsies, partial visual field deficits and seizures due to limited temporal lobe injury [43,56,65]. There were very few significant complications after the initial high-dose group of patients. After appropriate adjustments of dose schedules based on this early experience, focal temporal lobe necrosis and transient cranial nerve injury have been rare sequelae, in the range of 1% or less, and no other permanent therapeutic sequelae have occurred. A very low incidence of significant adverse sequelae has also been reported in patients treated with Bragg-peak proton irradiation at HCL-MGH and ITEP and with plateau-beam proton irradiation at INPh [25,28].

OTHER BENIGN TUMORS

Charged-particle irradiation has been applied to the treatment of a variety of benign intracranial tumors, including meningiomas, acoustic neuromas and craniopharyngiomas [38]. Selection criteria, treatment parameters and long-term clinical results in most cases have not yet been clearly defined. More-detailed follow-up evaluation is available for selected cohorts of patients with meningiomas.

Luchin et al [49] used proton-beam irradiation (two to four fractions; plateau-beam or Bragg-peak method) to treat 52 patients with cavernous sinus meningiomas. Maximum central doses of 50 to 70 Gy were used. With mean follow-up of 40.6 months (range, 13 to 77 months), local control was obtained in 84% of patients; five patients with inadequate dose-distribution in the tumor volume exhibited continued tumor growth.

Excellent local control has also been reported in patients treated with conventionally fractionated helium-ion irradiation for sphenoid ridge meningioma, where the optic nerves and/or chiasm were considered critical dose-limiting tissues. Tumor doses ranged from 53 to 80 GyE (mean, 63.5 GyE) (J. R. Castro, personal communication). The local control rate (minimum follow-up of 2 years) in a series of 24 patients was 88%; the 3-year Kaplan-Meier actuarial survival was 87%. This series includes patients with partially unresectable lesions or gross recurrences. While the range of follow-up extends to more than 8 years in some patients, the only failures occurred within 36 months of therapy in several early patients accepted for treatment with massive recurrent lesions. Treatment tolerance has been excellent.

MALIGNANT GLIOMAS

Malignant gliomas are among the human tumors that respond relatively poorly to conventional megavoltage irradiation. Treatment failures in resistant tumors can often be attributed, at least in part, to two factors: (1) tumor-dose limitations imposed by tolerance of adjacent normal tissues; and (2) intrinsic radioresistance of the tumor. Neon-ion irradiation has been proposed as a solution to both problems [46,71]. Neon-ion beams have the favorable dose-distribution characteristics of lighter charged-particle beams (see section on "Physical Properties of Charged-Particle Beams"), as well as the increased relative biologic effectiveness (RBE) associated with high linear energy transfer (LET). High-LET radiations include neutrons, pions and heavier-charged particles (e.g., neon ions). The dense ionization in tissue associated with these particles gives rise to several radiobiologic properties of potential value for the treatment of selected malignancies resistant to low-LET irradiation with protons and photons [3,8,65,71]. These properties include: (1) improved oxygen enhancement ratio, i.e., reduction of the radioresistance typical of hypoxic tumor cells; (2) decreased variation in the cell-cycle-specific radiosensitivity of tumor cells; (3) reduced ability of irradiated cells to repair potentially lethal and sublethal damage; and (4) diminished radioresistance attributable to cell-density or cell-contact effects. The increased RBE of high-LET radiation has been demonstrated by decreased cell survival in cultured mammalian cells and by reduced repair of radiation damage *in vitro* and *in vivo*.

The role of neon-ion irradiation in the treatment of malignant glioma is as yet undefined, and outcomes have thus far not been better than obtained with conventional irradiation. Preliminary studies have been limited to 16 patients treated with fractionated Bragg-peak neon-ion irradiation at the UCB-LBL Bevatron [8,46]. Because of limited availability of the neon-ion beam, most patients received mixed-beam treatments combining neon, helium and photon irradiation to bring total tumor doses to prescribed levels. Doses were calculated as gray-equivalent (GyE), using experimentally derived RBE factors which accounted for fraction size, type of tissue irradiated, beam energy, Bragg-peak width and biologic endpoint chosen [46]. In this formulation, neon RBE values ranged from 2.0 to 3.5, and helium RBE values ranged from 1.2 to 1.4.

Nine patients with glioblastoma (GBM) and seven with anaplastic astrocytoma (AA) received total equivalent doses ranging from 48.0 GyE to 69.0 GyE (median, 49.3 GyE), with neon physical doses ranging from 13.8 Gy to 25.0 Gy (median, 18.6 Gy) [46]. Follow-up ranged from 3 to 77 months. Local control was obtained in only one patient (with GBM) who died 31 months after treatment. The only patient surviving at the time of analysis had developed local recurrence of AA 25 months following treatment. Two patients treated solely with neon for GBM developed fatal radiation necrosis. One had received 54.4 GyE (assumed RBE, 2.43); the other patient died from combined local failure and brain necrosis (48.0 GyE; assumed RBE, 2.98). Although the acute skin reaction in each case was consistent with these assumed RBE values, the RBE for late brain necrosis was revised upward to a range of 4.0 to 4.5. It remains uncertain whether the potential benefits of high-LET irradiation for malignant gliomas will be realized.

VASCULAR MALFORMATIONS AND CAROTID-CAVERNOUS FISTULAE

More than 2,000 patients world-wide since 1965 have been treated with charged-particle radiosurgery for vascular malformations of the brain, primarily at UCB-LBL [16,17,18,39, 42,66,67,68], HCL-MGH [22,23,24], ITEP [58,59,61], and INPh [28,29,57]. Between 1980 and 1992, we treated 426 patients with intracranial vascular malformations using helium-ion beams, initially at the UCB-LBL 184-inch synchrocyclotron and subsequently at the

UCB-LBL Bevatron. This total includes 379 patients with angiographically demonstrable AVMs and 47 patients with AOVMs. The therapeutic goals of radiosurgery for the treatment of AVMs are to achieve: (1) reduction or elimination of intracranial hemorrhage; (2) stabilization or reversal of progressive neurologic dysfunction; (3) lower frequency of seizures; and (4) improvement in frequency and intensity of headaches. In this section, we describe the methods of patient selection and evaluation, and clinical and neuroradiologic outcome and complications in a cohort of 86 consecutive patients with angiographically demonstrable AVMs, who were treated between 1983 and 1988 through the collaborative LBL-SUMC radiosurgery program [66]. The results of other programs using proton radiosurgery for treatment of AVMs and carotid-cavernous fistulae are then discussed briefly, as is our experience with the helium-ion treatment of AOVMs.

Arteriovenous Malformations: Berkeley – Stanford Series

Patient Selection. In the LBL-SUMC patient series [66], there were 47 females and 39 males, ranging in age at the time of treatment from 9 to 69 years (mean, 33 years). Many patients presented with more than one symptom; 60 had hemorrhaged, 11 had neurologic deficits unassociated with hemorrhage, 35 had seizures, and 40 had headaches. Sixty patients (70%) were graded clinically (using the Drake [13] neurosurgical scale) as *excellent* before radiosurgery, 24 (28%) as *good*, and two (2%) as *poor*. Prior to radiosurgery, 17 patients had undergone partial resection of their AVMs, seven had flow-directed embolization, and five had both embolization and surgery. Nearly half of these patients (44%) had AVMs located in the brain stem, corpus callosum, thalamus or basal ganglia, and most of the remainder had large malformations in critical areas of the cerebrum — the sensory, motor, language, or visual areas of the cortex. Using *angiographic-volume* criteria (the volume of the parallelepiped enclosing the AVM target volume delineated on orthogonal stereotactic cerebral angiograms), the preradiosurgical volumes of the malformations were 0.33 to 288 cm^3; 25% of AVMs were larger than 25 cm^3.

Clinical Follow-Up and Outcome. Clinical evaluation, performed 24 to 72 months (mean, 38 months) after radiosurgery, found that 63% of patients presenting with seizures and 68% of patients presenting with headaches had improvement of these symptoms [66]. Of 11 patients presenting with progressive neurologic deficits unrelated to hemorrhage, there was improvement in 3 patients and stabilization of neurologic status in 6 patients. The mechanisms underlying the observed improvements in seizure activity and headache syndromes and the stabilization or improvement of progressive nonhemorrhagic neurologic dysfunction following radiosurgery are poorly understood. These changes appear to be associated, in large measure, however, with improved regional cerebral blood flow, stabilization of hemodynamic imbalance and reversal of vascular steal associated with progressive thrombosis of the malformation [16,66]. Table 1 shows the distribution of clinical grades for patients before radiosurgery and at most recent follow-up. Clinical outcome was *excellent* in 58% and *good* in 36% of all patients in the series.

Neuroradiologic Response. Cerebral angiography was performed at yearly intervals to evaluate postradiosurgical changes. In general, the observed patterns of response can be summarized as follows: (1) after a variable latency period, the likelihood of achieving complete AVM obliteration increases progressively over a period of about 3 years; (2) the probabilities of eventual AVM obliteration and adverse treatment sequelae both increase as the radiation dose increases; (3) the entire AVM must be thrombosed to achieve an optimal clinical outcome; and (4) favorable response is achieved more readily with smaller lesions. The first hemodynamic changes observed include a decrease in blood flow through the AVM, probably due to progressive obliteration of the small shunting vessels, with a decrease in size of the feeding arteries and draining veins. This stage is followed by a progressive decrease in the AVM volume until stabilization or complete obliteration of the AVM occurs. Many uncertainties remain regarding optimal radiosurgical treatment parameters for malformations of various sizes and locations in the brain [16,66] and the evolving role of embolization and/or microsurgery in combination with charged-particle radiosurgery [55,68].

The angiographic results 2 years after radiosurgery (Table 2) indicate that complete obliteration of the AVM occurred in 70%, partial obliteration (10 to 99% obliteration) in 23%, and no change in 7%. By 3 years after treatment, 90% of patients had complete AVM obliteration, 6% had partial obliteration, and 4% had no change. The rate and extent of obliteration appear to be threshold phenomena directly related to the AVM volume and the radiation dose. Smaller AVMs had higher rates of obliteration than larger ones ($p<0.005$ after 1 and 2 years, Mann-Whitney test). AVMs smaller than 4 cm^3 thrombosed more rapidly and more completely than larger lesions ($p<0.05$ for the comparison with AVMs 4 cm^3 to 25 cm^3 in volume and $p<0.001$ for the comparison with those >25 cm^3, Cox test) (Fig. 16). Intermediate-sized AVMs were obliterated more rapidly and more completely than large AVMs ($p<0.05$, Cox test).

Complete obliteration occurred more frequently in malformations treated with higher doses (30 to 45 GyE) ($p<0.05$ after 1 and 2 years, Mann-Whitney test) (Table 3). AVMs treated with intermediate doses (24 to 28 GyE) also responded well at 2 and 3 years. Preliminary results with the lowest-dose group (11.5 to 20 GyE) were encouraging after 3-year follow-up, but thus far the number of patients in this group is too small to permit firm conclusions.

Post-Treatment Hemorrhage. Ten of 86 patients (12%) have hemorrhaged from residual angiographically demonstrable AVMs after radiosurgery, 7 patients during the first year, and 3 thereafter [66]. Hemorrhage resulted in permanent new neurologic deficits in 3 patients and death in 2 patients; the other 5 patients recovered fully. AVMs in 7 of these 10 patients had bled before treatment. No patients with angiographic evidence of complete obliteration of the malformation hemorrhaged subsequently. Until complete obliteration occurs, patients remain at risk; one patient with 95% AVM obliteration hemorrhaged 34 months after treatment.

Complications and Sequelae. Serious early sequelae have been negligible following radiosurgery [16,39,40,66]. A few patients with a prior history of seizures had transiently increased seizure activity which was readily controlled by adjustment of anticonvulsant medications. A few patients who presented initially with severe headaches required increased doses of oral analgesics for a few days following treatment. No patients experienced nausea, vomiting or hyperpyrexia. No deaths have occurred from the irradiation procedure.

Several categories of delayed radiation injury have been observed [39,40,54,65]. On the basis of MRI, CT, angiography and clinical evaluation, the treatment-associated sequelae can be classified as white matter changes or vasculopathy and include vasogenic edema, occlusion of functional vasculature and radiation necrosis. The manifestations and incidence of clinical sequelae depend, in part, on the region of the brain involved, the volume of normal and abnormal brain tissue affected, the radiation dose, the presence of prior tissue injury from spontaneous hemorrhage or previous interventional procedures, and the timing and nature of therapeutic measures.

Clinical complications following radiosurgery were most common in patients with AVMs in the brain stem, thalamus or basal ganglia. About 20% of patients (17 of 86) experienced complications between 3 and 38 months after treatment (mean, 13.4 months). Seven patients had minor complications, such as visual field deficit, diplopia, unilateral hearing impairment, slight gait ataxia or mild paresis; three of them recovered completely and four partially. Ten patients (12%) had major complications, including hemiparesis, gait ataxia, cranial nerve palsies, partial aphasia or hypothalamic syndrome; two recovered fully, seven recovered partially, and one remained unchanged. Some patients had more than one complication. Hemiparesis was the most common major complication and visual field deficit was the most common minor complication.

In about half of all the patients (33 of 65) examined after radiosurgery with MRI and CT, deep-white-matter changes occurred between 4 and 26 months after treatment (mean, 15.3 months); 20 of these patients were asymptomatic. In the 13 patients who were clinically symptomatic, the white-matter changes had MRI and CT patterns consistent with those described following radiation-induced brain injury, viz., abnormal signals on MRI or low attenuation on CT scans. These findings usually were associated with an appreciable amount of cerebral edema. A biopsy of the involved white matter in one patient revealed areas of tissue necrosis. Of 13 symptomatic patients, changes observed on MRI and CT resolved partially in 11 patients, and completely in two patients. Radiation-induced vasculopathy occurred in three patients and was characterized by arterial stenosis or thrombosis on cerebral angiograms and by MRI and CT changes consistent with cerebral ischemia. Doses ranged from 25 to 45 GyE, delivered to *angiographic volumes* of 0.85 cm^3 to 40 cm^3.

Complications were more prevalent with higher doses and larger volumes of treated brain tissue (Fig. 17). Among the 20 patients who received doses above 25 GyE and whose angiographic volumes of treated tissue were more than 13 cm^3, 10 experienced major or minor complications; these represented almost 60% of all clinical complications. Complications were limited to the initial 46 patients treated in the higher-dose phase of the dose-searching protocol. None of the 40 patients in the series treated with lower doses in the later phases of the protocol experienced any complications during this last 5-year period since 1986.

Additional Therapy. In selected patients in whom radiosurgery has not achieved complete AVM obliteration within 3 years, we have carried out additional treatment with microsurgery, embolization, or both [55]. In three patients who underwent open surgery for residual AVMs several years after radiosurgery, we found the AVMs to be markedly less vascular and more easily resected than expected had the patient not received radiosurgery. In another patient whose AVM was not obliterated 3 years following radiosurgical treatment, we were able to achieve complete thrombosis of the AVM using endovascular embolization alone. It appears that the small-vessel component of the AVM had likely been obliterated by the radiosurgical treatment, and that embolization-induced occlusion of the limited number of residual fistulae was able to obliterate fully the remaining AVM shunts. Although our experience with helium-ion radiosurgery prior to open microsurgery and embolization is limited, this approach may prove useful in the multistage management of some unusually large and complex AVMs in which complete obliteration has not occurred by 3 years or more.

Partial-Volume Radiosurgery. Certain sequelae of the treatment procedure may arise from the hemodynamic alterations of the AVM as it undergoes obliteration [40]. The creation of high-flow shunting within the AVM may increase the probability of intracranial hemorrhage [47]. This is a potential hazard of any incomplete treatment. Undesirable shunts can be created acutely, by subtotal surgical excision or embolization, or subacutely, by limited focal irradiation (*partial-volume radiosurgery*). During the initial phase of our clinical protocol, a selected number of patients with large hemispheric AVMs were treated with stereotactic focal irradiation limited to the earliest-filling component of the arterial phase, that is, the so-called *nidus* of the AVM, rather than the entire angiographic arterial phase, that is, the complete AVM *core.* In many cases, this approach resulted in obliteration of the target volume, but the periphery of the malformation was left intact, thereby creating an undesirable shunt with attendant risks of hemorrhage. We no longer consider it acceptable to treat an AVM without encompassing its entire arterial phase with a homogeneous dose distribution. Those patients whose initial radiosurgical treatment failed to meet these criteria are re-evaluated and given additional treatment if residual AVM shunts persist.

Arteriovenous Malformations: Other Series

Kjellberg and associates [22,23,24] have used single-fraction Bragg-peak proton (160 MeV) therapy at HCL-MGH to treat more than 1,300 patients with vascular malformations of the brain (R. N. Kjellberg, personal communication). Irradiation generally is delivered with parallel opposed treatment fields. Doses (typically, 10 to 50 Gy) are selected according to diameter of the AVM, using a nomogram based on lesion size and complication rate in a large number of treated patients [24]. Findings of follow-up evaluation in 1,000 patients with AVMs, 2 to 24 years after treatment with proton-beam therapy, have been reported [23]. In 104 patients, the clinical outcome was unrelated to hemorrhage or proton-beam therapy.

Of the remaining 896 patients, 818 (91.3%) were the same or improved as compared to their neurologic status at the time of treatment; 27 (3%) had moderate deficits from hemorrhage or proton-beam therapy but functioned independently at pretreatment levels; seven (0.8%) had severe deficits and were dependent to varying degrees; two (0.2%) were vegetative; 39 (4.4%) were dead (37 from hemorrhage and two from treatment complications); three (0.3%) were lost to follow-up after surviving hemorrhage [23]. Analysis by actuarial life-table methods showed 98.4% 24-year survival for patients with AVMs ≤3 cm in diameter and 93% 24-year survival for all patients [23]; these data were contrasted to a 24-year survival of 77% reported for an untreated historical control group. Of the 37 patients who died from hemorrhage, 22 died within the first 2 years after treatment; 33 lethal hemorrhages occurred in patients with AVMs >3 cm in diameter. An additional 101 patients survived hemorrhage, including the three above-mentioned patients who were lost to follow-up. Complications of treatment occurred in 17 patients (6 months to 6.5 years after treatment), but only seven were in the last 925 patients following downward adjustments in treatment doses. In general, treatment doses used in this patient series were significantly lower than those used in the LBL-SUMC series described above.

Minakova and colleagues [58,59,61] have used Bragg peak proton radiosurgery at ITEP in 66 patients with AVMs (Ye. I. Minakova, personal communication). The Bragg peak is spread to a width of 15 to 25 mm as required; seven or eight beam ports are used. Single-fraction maximum doses of 30 to 50 Gy are used, depending on the size and location of the AVM; the periphery of the lesion is treated to the 50% isodose. Of 28 patients followed-up angiographically for 2 years after treatment, 71% demonstrated total or partial obliteration. Two patients sustained hemorrhage within the first year after treatment. Two patients experienced neurologic sequelae with corresponding CT findings of edema, the onset occurring in one patient at 22 months, and in the other, 18 months after radiosurgery (dose, 50 Gy; beam diameter, 20 mm). Both patients responded well to brief courses of high-dose steroids.

Konnov and co-workers [28,57] have used plateau-beam proton radiosurgery at LINPh to treat 187 patients with AVMs and 6 patients with arterial aneurysms (B. A. Konnov, personal communication). Of the first 148 AVM patients treated, embolization and partial surgical excision were performed in 18 patients and 16 patients, respectively. Using isocentrically directed converging irradiation arcs, maximal doses of 40 to 80 Gy were delivered to diameters of 5 to 10 mm; the irradiated-field size was defined by the extent of the 50% isodose contour [28]. Larger AVMs were treated with two isocenters. Five patients died from recurrent hemorrhage during the first year. Angiographic follow-up 1 to 8 years after treatment was obtained in 109 patients. Complete AVM obliteration was achieved in 23 of 36 patients (64%) with angiographically determined AVM volumes $\leq$2.0 cm^3, in 7 of 20 patients (35%) with 2.1- to 4.0-cm^3 AVMs, in 3 of 10 (30%) with 4.1- to 6.0-cm^3 AVMs, and in 1 of 43 (2%) with AVMs >6.0 cm^3 [57]. Nearly all cases of complete AVM obliteration occurred within the first 3 years after treatment. AVM obliteration and volume decrease were positively correlated with both average absorbed dose and dose to the margin of the treatment volume [57].

Carotid-Cavernous Fistulae

Stereotactic radiosurgery with plateau-beam proton irradiation has been used by Minakova and colleagues [29,58,59,61] to treat 24 patients with carotid-cavernous fistulae (Ye. I. Minakova, personal communication). Patients were treated with 40 to 60 Gy in one or two fractions, using 10- to 12-mm beams. Thus far, all patients have had regression of ocular symptoms and headaches, usually between 4 and 8 months after treatment. In four of eight patients examined, complete obliteration of the fistulae was observed on follow-up angiograms; three other patients had partial fistulae obliteration. No patient experienced adverse sequelae.

Angiographically Occult Vascular Malformations

Stereotactic radiosurgery of AOVMs presents complex problems in diagnosis, patient selection criteria, treatment planning, choice of dose, and criteria for clinical and neuroradiologic follow-up evaluation [39,42,67]. Since 1983 we have treated 47 patients with symptomatic AOVMs with stereotactic heavy-charged-particle Bragg peak radiosurgery (dose range, 8 to 45 GyE), using the helium-ion beams at the UCB-LBL 184-inch synchrocyclotron and Bevatron. There were 25 males and 22 females, ranging in age at the time of treatment from 13 to 64 years. Twenty-eight AOVMs (60%) were located in the brain stem, 15 (32%) in the thalamus, internal capsule or basal ganglia, three (6%) in the motor or language cortex, and one (2%) in the cerebellopontine angle. AOVMs measured between 0.1 cm^3 and 15.2 cm^3. Twenty-two patients (47%) were in *excellent* grade prior to treatment, 20 (43%) in *good* grade, and five (10%) in *poor* grade. There was clinical and radiologic evidence of hemorrhage in all patients; most had hemorrhaged repeatedly.

Clinical follow-up grade was *excellent* in 47% of patients, *good* in 34%, and *poor* in 9%; five patients (10%) died. Thirty-seven patients in *excellent* or *good* condition prior to treatment remained stable or improved neurologically. Two patients initially in *poor* condition, who had previously received conventional large-field radiotherapy (approximately 50 Gy) and chemotherapy for presumed brain stem glioma, died of disease progression 9 and 14 months after radiosurgical treatment; a third patient with a large hypothalamic AOVM who was initially in *good* condition deteriorated from recurrent hemorrhage 26 months after treatment and died 4 months later. These three patients had been treated with radiosurgical doses $\leq$10 GyE. A fourth patient initially in *poor* condition deteriorated markedly as a result of hemorrhage 13 months following treatment, and died with severe brain stem dysfunction 3 years later; she had been treated with a dose of 20 GyE. Another patient in *poor* condition prior to radiosurgery died 7 years after treatment (dose, 25 GyE) from recurrent hemorrhage.

Eight other patients had transient or permanent neurologic deterioration due to recurrent AOVM hemorrhage 2 months to 5 years after treatment (five within 13 months). Five of these patients recovered fully to their previous condition, including three following microsurgical resection of their AOVMs 20 months, 3 years and 5 years, respectively, after radiosurgery; histologic examination confirmed that these AOVMs were partially thrombosed [67]. The other three patients had permanent neurologic worsening following hemorrhage.

Seven of 47 patients (15%) with AOVMs had possible or probable treatment-associated sequelae 3 to 12 months after helium-ion radiosurgery; six of these patients had findings of enhanced signal on T2-weighted MRI. Two patients recovered fully without surgical treatment, three recovered to their baseline neurologic status following microsurgical resection of their AOVMs, and two patients had permanent worsening. Undetected recurrent hemorrhage or spontaneous thrombosis of adjacent vessels may have also contributed to neurologic deterioration in some of these patients.

Most patients demonstrated little change on sequential MRI scans over time, other than what could be explained by partial resorption or evolution of pre-existing hemorrhage [42]. No AOVM had associated radiologic findings comparable to those seen following radiosurgery for angiographically demonstrable AVMs, i.e., MRI findings typically associated with obliteration of abnormal vascular structures were not seen [39]. Follow-up CT scanning has been of limited value, other than for diagnosing acute recurrent hemorrhage where clinically suspected [42].

The clinical results following helium-ion radiosurgery for AOVMs are not as favorable as the results for high-flow AVMs [16,42,67]. Considerable clinical research is required to define more precisely the selection criteria for stereotactic radiosurgery in patients with AOVMs. The optimal treatment dose and radiosurgical target volume must be determined for the treatment of AOVMs in various locations within the brain. Neuroradiologic imaging methods are presently not able to demonstrate the vascular structures in most AOVMs or obliterative changes in response to radiosurgery. We have concluded that microsurgical resection should be the primary treatment for surgically accessible, symptomatic AOVMs. The potential value of helium-ion radiosurgery for surgically inaccessible AOVMs remains uncertain.

JUXTASPINAL TUMORS

The management of juxtaspinal and base-of-skull tumors (e.g., chordomas and chondrosarcomas) is a complex problem in neurosurgery and radiation oncology [2,7]. Complete surgical resection is uncommon, and most patients require post-operative irradiation. The proximity of these tumors to the spinal cord or brain stem, however, limits the radiation dose that can be delivered safely to the tumor with conventional radiotherapy techniques. Charged-particle radiotherapy delivered with conventional fractionation (60 to 75 GyE tumor dose, approximately 2 GyE per fraction) has been used with excellent results.

From 1978 through 1991, 85 patients with chordoma or chondrosarcoma of the cranial base or cervical spine were treated at LBL with helium-ion irradiation, most following subtotal surgical resection [2,6]. A minority of patients had received the first part of their radiation treatment with photons and were referred for helium-ion "boost" treatment; another group of patients was referred because of recurrent disease. Total helium-ion doses ranged from 36 to 80 GyE (mean, 67 GyE). Local control was obtained in 59 of 85 patients (70%) with a follow-up period ranging from 2 to 163 months (median, 34 months). The projected 5-year Kaplan-Meier actuarial survival was 67%; the actuarial survival and local control for these patients at 3 years were 70% and 68%, respectively. Patients treated for primary disease had a 78% actuarial local control rate at 2 years, whereas the rate for patients with recurrent disease was 33% [2]. Those patients with smaller tumor volumes (< 20 cm^3) had a significantly better local control rate than patients with larger tumor volumes (80% vs 33% actuarial rate at 5 years), as did patients whose radiation treatment was solely with charged particles. Local control was better for chondrosarcoma than for chordoma, and in the skull base than in the cervical spine. Serious complications included three patients with unilateral vision loss, two who became blind, and four with radiation injury to the brain stem.

Fractionated proton therapy has also proven successful for treatment of chordoma and chondrosarcoma of the base of skull; 5-year actuarial local control rates of about 80% have been reported [1,69]. By contrast, the local recurrence rate for these tumors following conventional photon irradiation is 64% [69].

OCULAR MELANOMAS

Several thousand patients in the United States and Europe have been treated for ocular melanoma using Bragg-peak irradiation with protons or helium ions (50 to 80 Gy) typically delivered in five fractions over 7 to 12 days [9,12,20,78]. In these clinical series, local control exceeding 95% has been achieved in selected patient groups, but distant metastases occurred in about 20% of patients. A large proportion of patients have maintained useful vision in the treated eye; however, enucleation due to complications has been required in 7% to 12% of patients.

SUMMARY

Charged-particle beams manifest unique physical properties which offer advantages for neurosurgery and radiation oncology. These properties include a finite range in tissue, a Bragg ionization peak and very sharp lateral edges. Charged-particle irradiation can be applied effectively using either the Bragg-peak method, where the charged particles *stop* within the target volume, or the plateau-beam method, where the charged particles pass completely through the patient's head. In either case, the target volume must be defined and located precisely within a reproducible three-dimensional frame of reference, the physical properties of the materials to be traversed by the beam must be determined accurately, and the patient must be positioned exactly with respect to the beam. Treatment planning consists of sequential stereotactic neuroradiologic imaging studies, computer-assisted correlations among the different types of imaging information and calculations of dose distribution.

Since 1954, more than 7,000 patients world-wide have been treated with charged-particle irradiation for various intracranial and juxtaspinal lesions. Most patients have been treated with single-dose irradiation or with a few large-dose fractions, but several hundred patients have been treated using conventional fractionation schedules. Therapeutic efficacy has been clearly demonstrated for the treatment of selected sites, e.g., pituitary adenomas, AVMs, juxtaspinal tumors and ocular melanomas. Optimal treatment parameters (dose, fractionation and choice of charged-particle species) have yet to be determined for lesions of varying histology, size and location. Improved three-dimensional treatment planning and beam delivery can be expected to improve cure rates and minimize adverse sequelae of treatment, especially for large or irregularly shaped lesions.

ACKNOWLEDGMENTS

The authors wish to thank Professors J. H. Lawrence (deceased), J. T. Lyman, C. A. Tobias, R. N. Kjellberg, Ye. I. Minakova, B. A. Konnov and Drs. M. H. Phillips, M. P. Marks, B. Lane and G. J. Candia for providing clinical research material and permission to describe their clinical and basic research. Research supported by Director, Office of Health and Environmental Research, U. S. Department of Energy under Contract No. DE-AC03-76SF00098.

References

[1] Austin-Seymour M, Munzenrider J, Goiten M, Verhey L, Urie M, Gentry R, Birnbaum S, Ruotolo D, McManus P, Skates S, Ojemann RG, Rosenberg A, Schiller A, Koehler A, Suit HD: Fractionated proton radiation therapy of chordoma and low-grade chondrosarcoma of the base of the skull. J Neurosurg 70:13–17,1989.

[2] Berson AM, Castro JR, Petti P, Phillips TL, Gauger G, Gutin P, Collier JM, Henderson SD, Baken K: Charged particle irradiation of chordoma and chondrosarcoma of the base of skull and cervical spine: The Lawrence Berkeley Laboratory experience. Int J Radiat Oncol Biol Phys 15:559–565, 1988.

[3] Blakely EA, Ngo FQH, Curtis SB, Tobias CA: Heavy-ion radiobiology: Cellular studies, in Lett JT (ed): *Advances in Radiation Biology (vol. 11)*. New York, Academic, 1984, pp 295–389.

[4] Bragg WH, Kleeman RD: On the ionization curves of radium. Philosoph Mag 8:726–738, 1904.

[5] Brobeck WM, Lawrence EO, MacKenzie KR, McMillan EM, Serber R, Sewell DC, Simpson KM, Thornton RL: Initial performance of the 184-inch cyclotron of the University of California. Phys Rev 71:449–450, 1947.

[6] Castro JR: High-LET charged particle radiotherapy, in Dewey W, Edington M, Fry RJM, Hall E, Whitmore G (eds): *Proceedings of the 9th International Congress of Radiation Research (vol. 2)*. New York, Academic, 1992, pp 635–640.

[7] Castro JR, Collier JM, Petti PL, Nowakowski V, Chen GTY, Lyman JT, Linstadt D, Gauger G, Gutin P, Decker M, Phillips TL, Baken K: Charged particle radiotherapy for lesions encircling the brain stem or spinal cord. Int J Radiat Oncol Biol Phys 17:477–484, 1989.

[8] Castro JR, Saunders WM, Austin-Seymour MM, Woodruff KH, Gauger G, Chen GTY, Collier JM, Phillips TL, Zink SR: A phase I-II trial of heavy charged particle irradiation of malignant glioma of the brain: A Northern California Oncology Group study. Int J Radiat Oncol Biol Phys 11:1795–1800, 1985.

[9] Char DH, Castro JR, Kroll SM, Irvine AR, Quivey JM, Stone RD: Five-year follow-up of helium ion therapy for uveal melanoma. Arch Ophthalmol 108:209–214, 1990.

[10] Chen GTY, Singh RP, Castro JR, Lyman JT, Quivey JM: Treatment planning for heavy ion radiotherapy. Int J Radiat Oncol Biol Phys 5:1809–1819, 1979.

[11] Constable JD, Lawrence JH, Born JL, Tobias CA, Ariotti PE, Sangalli FF, Carlson RC, Toch P: Effect of alpha particle hypophysectomy on disseminated cancer of male breast. J Am Med Assoc 174:1720–1723, 1960.

[12] Decker M, Castro JR, Linstadt DE, Char D, Petti PL, Quivey JM, Ahn D: Ciliary body melanoma treated with helium particle irradiation. Int J Radiat Oncol Biol Phys 19:243–247, 1990.

[13] Drake CG: Cerebral arteriovenous malformations: Considerations for and experience with surgical treatment in 166 cases. Clin Neurosurg 26:145–208, 1979.

[14] Fabrikant JI, Levy RP: Radiation therapy of pituitary tumors, in Selman WR (ed): *Neuroendocrinology.* Baltimore, Williams & Wilkins (in press).

[15] Fabrikant JI, Levy RP, Phillips MH, Frankel KA, Lyman JT: Neurosurgical applications of ion beams. Nucl Instrum Methods Phys Res B40/41:1376-1384, 1989.

[16] Fabrikant JI, Levy RP, Steinberg GK, Phillips MH, Frankel KA, Lyman JT, Marks MP, Silverberg GD: Charged-particle radiosurgery for intracranial vascular malformations. Neurosurg Clin North Am 3:99–139, 1992.

[17] Fabrikant JI, Lyman JT, Frankel KA: Heavy charged-particle Bragg peak radiosurgery for intracranial vascular disorders. Radiat Res [Suppl] 104:S244-S258, 1985.

[18] Fabrikant JI, Lyman JT, Hosobuchi Y: Stereotactic heavy-ion Bragg peak radiosurgery: Method for treatment of deep arteriovenous malformations. Br J Radiol 57:479–490, 1984.

[19] Frankel KA, Levy RP, Fabrikant JI, Phillips MH: Heavy-charged-particle radiosurgery: Rationale and method, in Alexander E, Loeffler JS, Lunsford LD (eds): *Stereotactic Radiosurgery*. New York, McGraw-Hill (in press).

[20] Gragoudas ES, Seddon JM, Egan K, Glynn R, Munzenrider J, Austin-Seymour M, Goiten M, Verhey L, Urie M, Koehler A: Long-term results of proton beam irradiated uveal melanomas. Ophthalmology 94:349–353, 1987.

[21] Hardy J: Transsphenoidal microsurgical treatment of pituitary tumors, in Linfoot JA (ed): *Recent Advances in the Diagnosis and Treatment of Pituitary Tumors*. New York, Raven, 1979, pp 375–388.

[22] Kjellberg RN: Stereotactic Bragg peak proton beam radiosurgery for cerebral arteriovenous malformations. Ann Clin Res 18 [Suppl 47]:17–19, 1986.

[23] Kjellberg RN, Candia GJ: Stereotactic proton beam therapy for cerebral AVMs. *Harvard Radiosurgery Update*, Chestnut Hill, MA, 1990 (Abstr).

[24] Kjellberg RN, Hanamura T, Davis KR, Lyons SL, Adams RD: Bragg peak proton-beam therapy for arteriovenous malformations of the brain. N Engl J Med 309:269–274, 1983.

[25] Kjellberg RN, Kliman B: Lifetime effectiveness - A system of therapy for pituitary adenomas, emphasizing Bragg peak proton hypophysectomy, in Linfoot JA (ed): *Recent Advances in the Diagnosis and Treatment of Pituitary Tumors*. New York, Raven, 1979, pp 269–288.

[26] Kjellberg RN, McMeel JW, McManus NL, Koehler AM: Pituitary suppression in diabetic retinopathy by proton beam in surgically "unfit" patients, in Goldberg MF,

Fine SL (eds): *Symposium on the Treatment of Diabetic Retinopathy. Airlie House, Warrenton, VA.* Arlington, U S Public Health Service (Publication No. 1890), 1968, pp 249–276.

[27] Kjellberg RN, Shintani A, Franzt AG, Kliman B: Proton beam therapy in acromegaly. N Engl J Med 278:689–695, 1968.

[28] Konnov B, Melnikov L, Zargarova O, Lebedeva L, Yalynych N, Karlin D: Narrow proton beam therapy for intracranial lesions, in Heikkinen E, Kiviniitty K (eds): *International Workshop on Proton and Narrow Photon Beam Therapy.* Oulu, Finland, University of Oulu, 1989, pp 48–55.

[29] Krymsky VA, Serbinenko FA, Minakova YeI, Luchin YeI, Lysacheva AG, Nekipelov EF, Klyuchnikov SI: Proton beam irradiation of spontaneous arteriosinusal anastomoses of the cavernous sinus area. Med Radiol (Mosk) 32(8):57–61, 1987 (in Russian).

[30] Lawrence JH: Heavy particle irradiation of intracranial lesions, in Wilkens RH, Rengachary SS (eds): *Neurosurgery.* New York, McGraw-Hill, 1985, pp 1113–1132.

[31] Lawrence JH: Proton irradiation of the pituitary. Cancer 10:795–798, 1957.

[32] Lawrence JH, Born JL, Tobias CA, Carlson R, Sangalli F, Welch G: Clinical and metabolic studies in patients after alpha particle subtotal or total hypophysectomy, in *Medicine in Japan in 1959. Proceedings of the 15th General Assembly of the Japan Medical Congress (vol. 5).* Tokyo, 1959, pp 859–862.

[33] Lawrence JH, Linfoot JA: Treatment of acromegaly, Cushing disease and Nelson syndrome. West J Med 133:197–202, 1980.

[34] Lawrence JH, Tobias CA, Born JL, Linfoot JH, D'Angio GJ: Heavy particles in experimental medicine and therapy. J Am Med Assoc 196:152–156, 1966.

[35] Lawrence JH, Tobias CA, Born JL, Wang CC, Linfoot JH: Heavy-particle irradiation in neoplastic and neurologic disease. J Neurosurg 19:717–722, 1962.

[36] Lawrence JH, Tobias CA, Linfoot JA, Born JL, Gottschalk A, Kling RP: Heavy particles, the Bragg curve and suppression of pituitary function in diabetic retinopathy. Diabetes 12:490–501, 1963.

[37] Levy RP, Fabrikant JI: Medical applications of stereotactic radiosurgery, in Phillips MH (ed): *Physical Aspects of Stereotactic Radiosurgery.* New York, Plenum, 1993, pp 259–300.

[38] Levy RP, Fabrikant JI, Frankel KA, Phillips MH, Lyman JT: Charged-particle radiosurgery of the brain. Neurosurg Clin North Am 1:955–990, 1990.

[39] Levy RP, Fabrikant JI, Frankel KA, Phillips MH, Lyman JT: Stereotactic heavy-charged-particle Bragg peak radiosurgery for the treatment of intracranial arteriovenous malformations in childhood and adolescence. Neurosurgery 24:841–852, 1989.

[40] Levy RP, Fabrikant JI, Frankel KA, Phillips MH, Steinberg GK, Marks MP, DeLaPaz RL, Chuang FYS: Clinical-radiological evaluation of sequelae of stereotactic radiosurgery for intracranial arteriovenous malformations, in Steiner L (ed): *Radiosurgery: Baselines and Trends.* New York, Raven, 1992, pp 209–220.

[41] Levy RP, Lo EH, Fabrikant JI: Biologic basis for stereotactic radiosurgery, in Phillips MH (ed): *Physical Aspects of Stereotactic Radiosurgery.* New York, Plenum, 1993, pp 205–257.

[42] Levy RP, Steinberg GK, Fabrikant JI, Frankel KA, Phillips MH, Marks MP: Stereotactic heavy-charged-particle radiosurgery for angiographically occult vascular malformations, in Lunsford LD (ed): *Stereotactic Radiosurgery Update.* New York, Elsevier, 1992, pp 177–183.

[43] Linfoot JA: Heavy ion therapy: Alpha particle therapy of pituitary tumors, in Linfoot JA (ed): *Recent Advances in the Diagnosis and Treatment of Pituitary Tumors.* New York, Raven, 1979, pp 245–267.

[44] Linfoot JA, Born JL, Garcia JF, Manougian E, Kling RP, Chong CY, Tobias CA, Carlson RA, Lawrence JH: Metabolic and ophthalmological observations following heavy particle pituitary suppressive therapy in diabetic retinopathy, in Goldberg MF, Fine SL (eds): *Symposium on the Treatment of Diabetic Retinopathy. Airlie House, Warrenton, VA*. Arlington, U S Public Health Service (Publication No. 1890), 1968, pp 277–289.

[45] Linfoot JA, Lawrence JH, Born JL, Tobias CA: The alpha particle or proton beam in radiosurgery of the pituitary gland for Cushing's disease. N Engl J Med 269:597–601, 1963.

[46] Linstadt DE, Castro JR, Phillips TL: Neon ion radiotherapy: Results of phase I/II clinical trial. Int J Radiat Oncol Biol Phys 20:761–769, 1991.

[47] Lo EH, Fabrikant JI, Levy RP, Phillips MH, Frankel KA, Alpen EL: An experimental compartmental flow model for assessing the hemodynamic response of intracranial arteriovenous malformations to stereotactic radiosurgery. Neurosurgery 28:251–259, 1991.

[48] Lopatkin NA, Khazanov VG, Minakova YeI, Krymsky VA: Proton irradiation of the hypophysis in the combined antiandrogenical treatment of cancer of the prostate. Khirurgiia (Sofiia) 3:1–3, 1988 (in Bulgarian).

[49] Luchin YI, Minakova YeI, Krymsky VA: Proton beam irradiation of cavernous sinus meningiomas, in Heikkinen E, Kiviniitty K (eds): *International Workshop on Proton and Narrow Photon Beam Therapy*. Oulu, Finland, University of Oulu, 1989, pp 99–100.

[50] Luft R: The use of hypophysectomy in juvenile diabetes mellitus with vascular complications. Diabetes 11:461–462, 1962.

[51] Lyass FM, Minakova YeI, Rayevskaya SA, Krymsky VA, Luchin YeI, et al: The role of radiotherapy in the treatment of pituitary adenomas. Med Radiol (Mosk) 34 (8):12–24, 1989 (in Russian).

[52] Lyman JT, Chong CY: ISAH: A versatile treatment positioner for external radiation therapy. Cancer 34:12–16, 1974.

[53] Lyman JT, Phillips MH, Frankel KA, Fabrikant JI: Stereotactic frame for neuroradiology and charged particle Bragg peak radiosurgery of intracranial disorders. Int J Radiat Oncol Biol Phys 16:1615–1621, 1989.

[54] Marks MP, DeLaPaz RL, Fabrikant JI, Frankel KA, Phillips MH, Levy RP, Enzmann DR: Imaging of charged-particle stereotactic radiosurgery for intracranial vascular malformations. Part II. Complications. Radiology 168:457–462, 1988.

[55] Marks MP, Lane B, Steinberg GK, Fabrikant JI, Levy RP, Frankel KA, Phillips MH: Endovascular treatment of cerebral AVMs following radiosurgery. Am J Neuroradiol (in press).

[56] McDonald LW, Lawrence JH, Born JL, Lyman JT: Delayed radionecrosis of the central nervous system, in Lawrence JH (ed): *Semiannual Report. Biology and Medicine. Donner Laboratory and Donner Pavilion. Fall 1967.* Berkeley, Regents of the University of California, Report UCRL-18066, 1967, pp 173–192.

[57] Melnikov LA, Konnov BA, Yalynych NN: Radiosurgery of cerebral AVM, in Heikkinen E, Kiviniitty K (eds): *International Workshop on Proton and Narrow Photon Beam Therapy.* Oulu, Finland, University of Oulu, 1989, pp 92–98.

[58] Minakova YeI: Review of twenty years proton therapy clinical experience in Moscow, in *Proceedings of the Second International Charged Particle Workshop.* Loma Linda, CA, 1987, pp 1–23.

[59] Minakova YeI: Twenty years clinical experience of narrow proton beam therapy in Moscow, in *Proceedings of the International Heavy Particle Therapy Workshop*. Paul Scherrer Institute, Villigen, Switzerland, 1990, pp 158–162.

[60] Minakova YeI, Kirpatovskaya LYe, Lyass FM, Snigiryova RYa, Krymsky VA: Proton therapy of pituitary adenomas. Med Radiol (Mosk) 28 (10):7–13, 1983 (in Russian).

[61] Minakova YeI, Krymsky VA, Luchin YeI, Serbinenko FA, Lyass FM, Gabibov GA: Proton beam therapy in neurosurgical clinical practice. Med Radiol (Mosk) 32 (8):36–42, 1987 (in Russian).

[62] Minakova YeI, Vasil'eva NN, Svyatukhina OV: Irradiation of the hypophysis with single large dose of high energy protons for advanced breast carcinoma. Med Radiol (Mosk) 22 (1):33–39, 1977 (in Russian).

[63] Phillips MH, Frankel KA, Lyman JT, Fabrikant JI, Levy RP: Comparison of different radiation types and irradiation geometries in stereotactic radiosurgery. Int J Radiat Oncol Biol Phys 18:211–220, 1990.

[64] Phillips MH, Frankel KA, Lyman JT, Fabrikant JI, Levy RP: Heavy-charged particle stereotactic radiosurgery: Cerebral angiography and CT in the treatment of intracranial vascular malformations. Int J Radiat Oncol Biol Phys 17:419–426, 1989.

[65] Rodriguez A, Levy RP, Fabrikant JI: Experimental central nervous system injury after charged-particle irradiation, in Gutin PH, Leibel SA, Sheline GE (eds): *Radiation Injury to the Nervous System*. New York, Raven, 1991, pp 149–182.

[66] Steinberg GK, Fabrikant JI, Marks MP, Levy RP, Frankel KA, Phillips MH, Shuer LM, Silverberg GD: Stereotactic heavy-charged-particle Bragg-peak radiation for intracranial arteriovenous malformations. N Engl J Med 323:96–101, 1990.

[67] Steinberg GK, Levy RP, Fabrikant JI, Frankel KA, Phillips MH, Marks MP: Stereotactic helium ion Bragg peak radiosurgery for angiographically occult intracranial vascular malformations. Stereotact Funct Neurosurg 57:64–71, 1991.

[68] Steinberg GK, Levy RP, Marks MP, Fabrikant JI: Vascular malformations: Charged-particle radiosurgery, in Alexander E, Loeffler JS, Lunsford LD (eds): *Stereotactic Radiosurgery*. New York, McGraw-Hill (in press).

[69] Suit HD, Goitein M, Munzenrider J, Verhey L, Davis KR, Koehler A, Linggood R, Ojemann RG: Definitive radiation therapy for chordoma and chondrosarcoma of base of skull and cervical spine. J Neurosurg 56:377–385, 1982.

[70] Tobias CA: Pituitary radiation: Radiation physics and biology, in Linfoot JA (ed): *Recent Advances in the Diagnosis and Treatment of Pituitary Tumors*. New York, Raven, 1979, pp 221–243.

[71] Tobias CA, Alpen EL, Blakely EA, Castro JR, Chatterjee A, Chen GTY, Curtis SB, Howard J, Lyman JT, Ngo FQH: Radiobiological basis for heavy-ion therapy, in Abe M, Sakamoto K, Phillips TL (eds): *Treatment of Radioresistant Cancers*. Amsterdam, Elsevier, 1979, pp 159–183.

[72] Tobias CA, Anger HO, Lawrence JH: Radiologic use of high energy deuterons and alpha particles. Am J Roentgenol Radium Ther Nucl Med 67:1–27, 1952.

[73] Tobias CA, Lawrence JH, Born JL, McCombs RK, Roberts JE, Anger HO, Low-Beer BVA, Huggins CB: Pituitary irradiation with high-energy proton beams: A preliminary report. Cancer Res 18:121–134, 1958.

[74] Tobias CA, Roberts JE, Lawrence JH, Low-Beer BVA, Anger HO, Born JL, McCombs R, Huggins CB: Irradiation hypophysectomy and related studies using 340-MeV protons and 190-MeV deuterons, in *Proceedings of the International Conference on the*

Peaceful Uses of Atomic Energy (vol. 10). New York, United Nations Publications, 1956, pp 95–106.

[75] Verhey L, Goitein M: Problems of inhomogeneities in particle beam therapy, in Skarsgard LD (ed): *Pion and Heavy-Ion Radiotherapy. Pre-Clinical and Clinical Studies.* New York, Elsevier, 1983, pp 159–168.

[76] Wilson RR: Radiological use of fast protons. Radiology 47:487–491, 1946.

[77] Woodruff KH, Lyman JT, Lawrence JH, Tobias CA, Born JL, Fabrikant JI: Delayed sequelae of pituitary irradiation. Hum Pathol 15:48–54, 1984.

[78] Zografos L, Bercher L, Egger E, Chamot L, Gailloud C, Uffer S, Perret C, Markovits C: Treatment of eye tumors by accelerated proton beams. Seven years experience. Klin Mbl Augenheilk 200:431–435, 1992 (in French).

Figure Legends

Figure 1. Relative dose in water as a function of depth is shown for 8-MeV photons (dotted line), an *unmodulated* helium-ion (165 MeV/u) beam (solid line) and a helium-ion beam with a spread-out Bragg peak (SOBP) *modulated* to 2-cm width (dashed line) by interposing variable-thickness absorbers in the beam path. The unmodulated Bragg peak produces a narrow beam with high energy deposition at the end of the range, suitable for producing small intracranial lesions. For most radiosurgical applications, it is necessary to spread-out the width of the Bragg peak to ensure optimum dose distribution throughout the lesion. (*From* RP Levy [38].)

[XBL 901-331A]

Fig. 2. The Bragg ionization curve and its transverse profile for the 165-MeV/u helium-ion beam at the UCB-LBL Bevatron. **Left**, the Bragg-peak-to-plateau dose ratio is approximately three, and the relative biologic effectiveness in the peak is estimated to be about 1.3; thus, the biologic effect in the peak is about four times that in the plateau region. Dose fall-off from 90% to 10% occurs within 2 to 3 mm distal to the Bragg peak. **Right**, the transverse profile of the Bragg peak demonstrates sharp edges; the lateral dose fall-off from 90% to 10% occurs within 2.5 mm. This profile was measured 1 cm proximal to the distal edge of a beam with a 7-cm residual range and with the Bragg peak spread 2 cm. Distal and lateral dose fall-off are negligibly affected by spreading the Bragg peak. (*From* JI Fabrikant [16].)

[XBL 9012-3874]

Fig. 3. Charged-particle beams can be readily contoured by metal apertures shaped to conform to the cross-sectional size and shape of the target volume in any projection. **Upper**, a lateral projection view of a stereotactic cerebral angiogram (left internal carotid artery injection) demonstrates a large AVM occupying the genu and body of the corpus callosum. The composite radiosurgical target, selected after evaluation of the multivessel

cerebral angiogram study, has been outlined (see arrowheads). **Lower**, an individually tailored brass and cerrobend (a low-melting-temperature dense alloy) aperture has been fabricated from computer-defined contours derived from the cerebral angiogram to conform to the radiosurgical target. The aperture is inserted into the beam line for appropriate shaping of the lateral beams during radiosurgery (cf Fig. 5). (*From* RP Levy [38].)

[XBB 901-795A]

Fig. 4. Schematic diagram of charged-particle-beam delivery system at UCB-LBL for stereotactic radiosurgery of intracranial tumors and vascular disorders. The stereotactic patient-positioning system (ISAH) allows translation along three orthogonal axes (x,y,z) and rotation about the y and z axes, thereby providing precise patient immobilization and positioning for stereotactically directed charged-particle-beam therapy. The width of the high-dose Bragg ionization peak within the brain can be spread to the prescribed size by interposing a modulating filter of comparable maximum thickness (x cm) in the beam path, schematically shown here as a variable-thickness propeller. The range in tissue of the Bragg-peak region is determined by a range-modifying absorber. At the Bevatron accelerator, the range and modulation of the Bragg peak are controlled by use of a variable-position water-column absorber. An individually designed aperture, specifically tailored to the size and configuration of the intracranial lesion, shapes the beam in cross-section. Tissue-equivalent compensators further improve the precision placement of the high-dose Bragg-peak region by adjusting for irregular target contours, skull curvature and tissue inhomogeneities. Ion chambers monitor the dose delivered in each beam. (*From* RP Levy [39].)

[XBL 8810-7674]

Fig. 5. Stereotactic frame and patient mask system (cf Fig. 4). The head-immobilization mask is formed of thermoplastic material, and it is molded individually for each patient's head. Letters denote components of the stereotactic frame: (A) Top cross member. (B) Yoke. (C) Graphite support bar with fiducial marker. An identical bar is present on the

other side of the frame. (D) Sideplates with fiducial markers. The clear lucite sideplates have two grooves machined at right angles. Fine copper wires cemented into the grooves are imaged on lateral radiographs and serve as markers for angiograms and CT. For MRI, fine tubes filled with olive oil are substituted into the grooves. (E) Arch with fiducial markers. The arch supports two copper wire markers (or oil-tube markers for MRI) that are imaged on anteroposterior radiographs. (F) Positioning pins. (*From* JT Lyman [53].)

[CBB 877-5479A "with overlay"]

Fig. 6. Stereotactic helium-ion Bragg-peak radiosurgery treatment plan for a 29-year-old woman with a symptomatic angiographically occult vascular malformation in the pons. **Left (upper** and **lower)**, diagnostic stereotactic MRI scans in the axial and sagittal planes are used to define the target volume (ring of white dots) for stereotactic radiosurgery. **Middle (upper** and **lower)**, the target contour data are then transferred to corresponding stereotactic CT images for treatment planning and calculation of isodose contours for display. **Right (upper** and **lower)**, the isodose-contour information is then transferred back to the original MRI scans to permit the explicit demonstration (and modification, where required) of isodose-contour distributions in all desired anatomic planes. Isodose contours displayed here in the axial and sagittal planes are calculated for 10, 50, 70 and 90% of the maximum central dose. (*From* JI Fabrikant [16].)

[XBB 898-7352]

Fig. 7. Computer-reformatted overlay of digitized angiographic films for treatment-planning procedures, used to transfer the three-dimensional target volume for dose localization and to align the patient for the radiosurgical procedure. The overlay maps target contours, midplane bony landmarks, fiducial markers from the stereotactic frame and the isocenter of the patient positioner (denoted by the cross). **Upper**, lateral and anteroposterior views demonstrate the relative orientation of these elements when the stereotactic frame center is located at the isocenter of ISAH (**upper left**). **Lower**, corresponding views

demonstrate the relative orientation when the patient has been moved so as to place the center of the lesion at the isocenter of the immobilization system ("treatment position"). The two concentric target contours reflect the angiographically derived target contour magnified to match the localization radiograph (outer contour) and the actual size of the AVM (inner contour), respectively. (*From* MH Phillips [64].)

[XBL 888-2832]

Fig. 8. Stereotactic helium-ion Bragg-peak radiosurgery treatment plan for a 12-year-old girl with an AVM of the brain stem (inner ring of white dots). Isodose contours have been calculated at 10, 50, 80 and 100% of the maximum dose in the axial (**left**) and coronal (**right**) planes. The 100% contour conforms precisely to the periphery of the lesion. There is a very rapid fall-off in dose outside the AVM target volume. Since four noncoplanar beams are used, very little normal brain tissue receives even as much as 10% of the dose to the AVM and most of the brain receives no radiation at all. There is virtually complete sparing and protection of midbrain and pontine structures. The helium-ion beam was collimated by an elliptical brass aperture measuring 8.5 x 11.5 mm; treatment was performed using four ports in 1 day, to a volume of 0.3 cm^3 (dose, 25 GyE). (*From* RP Levy [39].)

[XBB 885-5361A]

Fig. 9. Stereotactic helium-ion Bragg-peak radiosurgery treatment plan for a large (54 cm^3) left temporal and deep central nuclei AVM in a 39-year-old man. **Left**, axial plane; **right**, sagittal plane. The helium-ion beam was collimated by 61 x 50 mm and 55 x 42 mm individually shaped brass and cerrobend apertures; 27 GyE was delivered in 3 days to the lesion (defined by the ring of white dots) using four noncoplanar beams. Isodose contours have been calculated for 10, 30, 50, 70, 90 and 99% of the maximum dose. The 90% isodose contour borders precisely on the periphery of the lesion. There is rapid dose fall-off to the 70% level, and the 10% isodose contour completely spares irradiation of the contralateral hemisphere. (*From* JI Fabrikant [16].)

[XBB 878-6973A]

Fig. 10. Stereotactic positioning table and head holder for plateau-beam helium-ion pituitary-irradiation system developed at the UCB-LBL 184-inch synchrocyclotron. The mask is a rigid transparent polystyrene unit which is tailored for each patient. During irradiation, the patient is positioned sequentially at 12 discrete angles, covering a 66° arc around the vertical (y) axis; at each position, the patient's head is turned in pendulum motion through a 70° arc around the horizontal (x) axis. (*From* RP Levy [38].)

[JHL 2897-C "with overlay"]

Fig. 11. Three-dimensional isodose contours for one octant of the radiation field used to treat pituitary adenomas at the UCB-LBL 184-inch synchrocyclotron. Stereotactic irradiation is performed with the plateau-ionization portion of the 230 MeV/u helium-ion beam. The dose fall-off from 90% to 10% occurs in less than 4 mm in the frontal plane. The technique produces very favorable dose distributions for the treatment of small intracranial lesions. (*From* JH Lawrence [30].)

[MU-14976]

Fig. 12. Autopsy specimen of the pituitary gland of a patient with metastatic breast carcinoma 14 years after stereotactic helium-ion radiosurgery performed for hormonal suppression. The central coagulative necrosis and the sharply defined peripheral rim of functioning pituitary gland are seen. (*From* JI Fabrikant [15].)

[CBB 762-1381]

Fig. 13. Median plasma human growth hormone (hGH) levels in 234 patients with acromegaly treated with stereotactic plateau-beam helium-ion radiosurgery. The numbers of patients used to calculate the median plasma levels before radiosurgery and for each time interval thereafter are shown at the top of the graph. Fourteen patients did not have pretreatment hGH measurements, but their hGH levels measured 4 to 18 years after

radiosurgery were comparable with those of the other 220 patients. The 20 patients in the series who subsequently underwent pituitary surgery or additional pituitary irradiation were included until the time of the second procedure. (*From* JH Lawrence [30].)

[XBL 829-4115]

Fig. 14. Pre- and post-treatment levels (mean ± SEM) of urinary fluorogenic corticosteroids (**upper**) and plasma cortisol (**lower**) are shown for Cushing's disease patients treated with helium-ion radiosurgery. Normal levels of plasma and urinary cortisols were achieved 1 year after treatment and these levels were maintained for at least 10 years follow-up. The number of patients studied at each time is shown in parentheses. (*From* JA Linfoot [43].)

[XBL 915-1090]

Fig. 15. Fasting plasma prolactin levels are shown before treatment and 1 year following helium-ion radiosurgery for females (**left**) and males (**right**) with prolactin-secreting tumors. A marked decrease in prolactin, usually to normal levels (dashed line), was observed in many patients at 1 year (*) post-treatment. Percent change is shown in parentheses. (*From* JA Linfoot [43].)

[XBL 915-1093]

Fig. 16. Kaplan-Meier cumulative plots illustrate the temporal pattern of complete AVM obliteration as a function of AVM size prior to helium-ion radiosurgery in 71 patients with angiographic follow-up. Solid line, pretreatment angiographic volumes <4 cm^3 (23 patients); dashed line, volumes 4 cm^3 to 25 cm^3 (28 patients); dotted line, volumes >25 cm^3 (20 patients). Vertical lines represent patients with residual AVM. Smaller lesions obliterate most frequently and with the shortest latency intervals. (*From* GK Steinberg [68].)

Fig. 17. The frequency of clinical complications (major and minor) following helium-ion

radiosurgery in relation to treatment dose and volume of treated AVM in 86 patients. The maximum doses (ordinate) and treatment volumes (abscissa) are given; the 90% isodose surface was contoured to the periphery of the target volume. Open circles, patients with complications; solid circles, patients with no complications. (*Adapted from* GK Steinberg [66].)

[XBL 926-1278]

Table 1. Clinical outcome in 86 patients after stereotactic radiosurgery

	Before Treatment		After Treatment	
Overall Outcome	n	(%)	n	(%)
Grade[a]				
Excellent	60	(70)	50	(58)
Good	24	(28)	31	(36)
Poor	2	(2)	2	(2)
Dead			3	(3)

Adapted with permission from GK Steinberg et al [66].

[a] Drake [13] neurosurgical scale.

Table 2. Number of patients with angiographically detectable obliteration of their lesions after stereotactic radiosurgery, according to volume of AVM before treatment

Volume (cm^3)[a]	Degree of obliteration						
	complete		partial[b]		no change		total
	n	(%)	n	(%)	n	(%)	n
After 1 year (11-13 months)							
<4	9	(53)	7	(41)	1	(6)	17
4-25	7	(29)	12	(50)	5	(21)	24
>25	1	(6)	15	(83)	2	(11)	18
All	17	(29)	34	(58)	8	(13)	59
After 2 years (24-27 months)							
<4	17	(94)	1	(6)	0		18
4-25	15	(75)	3	(15)	2	(10)	20
>25	8	(42)	9	(47)	2	(11)	19
All	40	(70)	13	(23)	4	(7)	57
After >3 years (>36 months)							
<4	18	(100)	0		0		18
4-25	19	(95)	0		1	(5)	20
>25	11	(73)	3	(20)	1	(7)	15
All	48	(90)	3	(6)	2	(4)	53

Adapted with permission from GK Steinberg et al [66].

[a] 4 cm^3 volume equals approximately 2.0-cm diameter sphere; 25 cm^3 volume equals approximately 3.7-cm diameter sphere.

[b] Denotes a 10-99% reduction in volume as detected angiographically.

Table 3. Number of patients with angiographically detectable obliteration of their lesions after stereotactic radiosurgery, according to treatment dose

Dose, GyE[a]	Degree of obliteration						
	complete		partial[b]		no change		total
	n	(%)	n	(%)	n	(%)	n
After 1 year (11-13 months)							
11.5-20	3	(17)	10	(56)	5	(27)	18
24-28	5	(20)	18	(72)	2	(8)	25
30-45	9	(56)	6	(38)	1	(6)	16
After 2 years (24-27 months)							
11.5-20	6	(50)	4	(33)	2	(17)	12
24-28	18	(67)	8	(29)	1	(4)	27
30-45	16	(89)	1	(6)	1	(6)	18
After >3 years (> 36 months)							
11.5-20	8	(100)	0		0		8
24-28	20	(87)	2	(9)	1	(4)	23
30-45	20	(95)	0		1	(5)	21

Adapted with permission from GK Steinberg et al [66].

[a] 1 GyE equals physical dose in Gy (100 rads) multiplied by a relative biologic effectiveness of 1.3 for the Bragg ionization peak of helium ions.

[b] Denotes a 10-99% reduction in volume as detected angiographically.

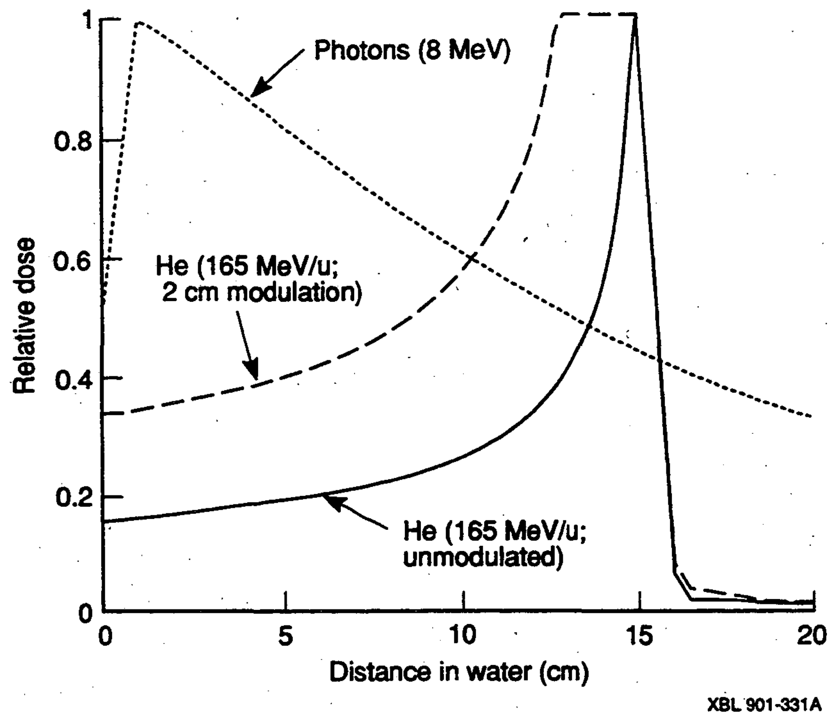
Photons (8 MeV)
He (165 MeV/u; 2 cm modulation)
He (165 MeV/u; unmodulated)
Relative dose
0
0.2
0.4
0.6
0.8
1
0
5
10
15
20
Distance in water (cm)
XBL 901-331A

Fig. 1

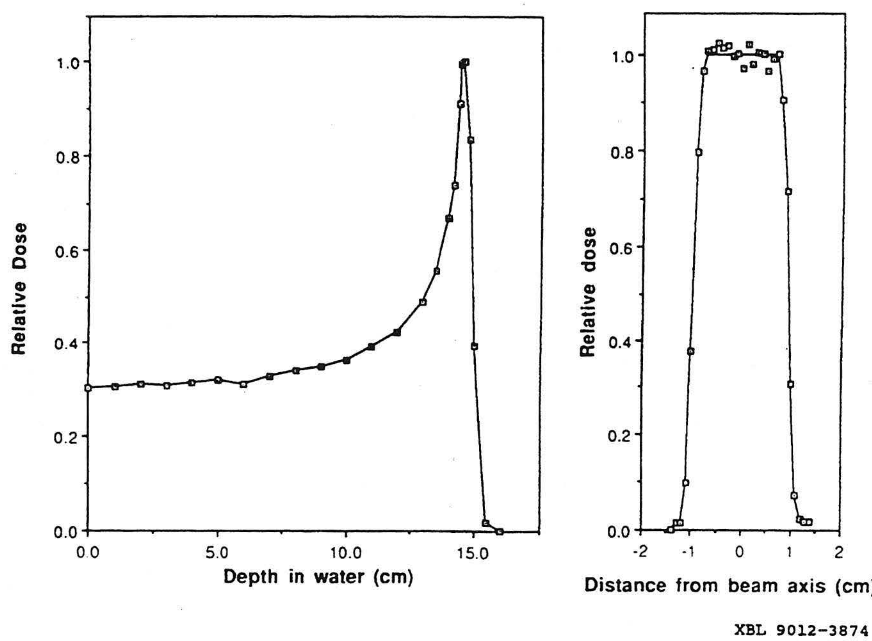
1.0
0.8
0.6
0.4
0.2
0.0
Relative Dose
0.0
5.0
10.0
15.0
Depth in water (cm)
1.0
0.8
0.6
0.4
0.2
0.0
Relative dose
-2
-1
0
1
2
Distance from beam axis (cm)
XBL 9012-3874

Fig. 2

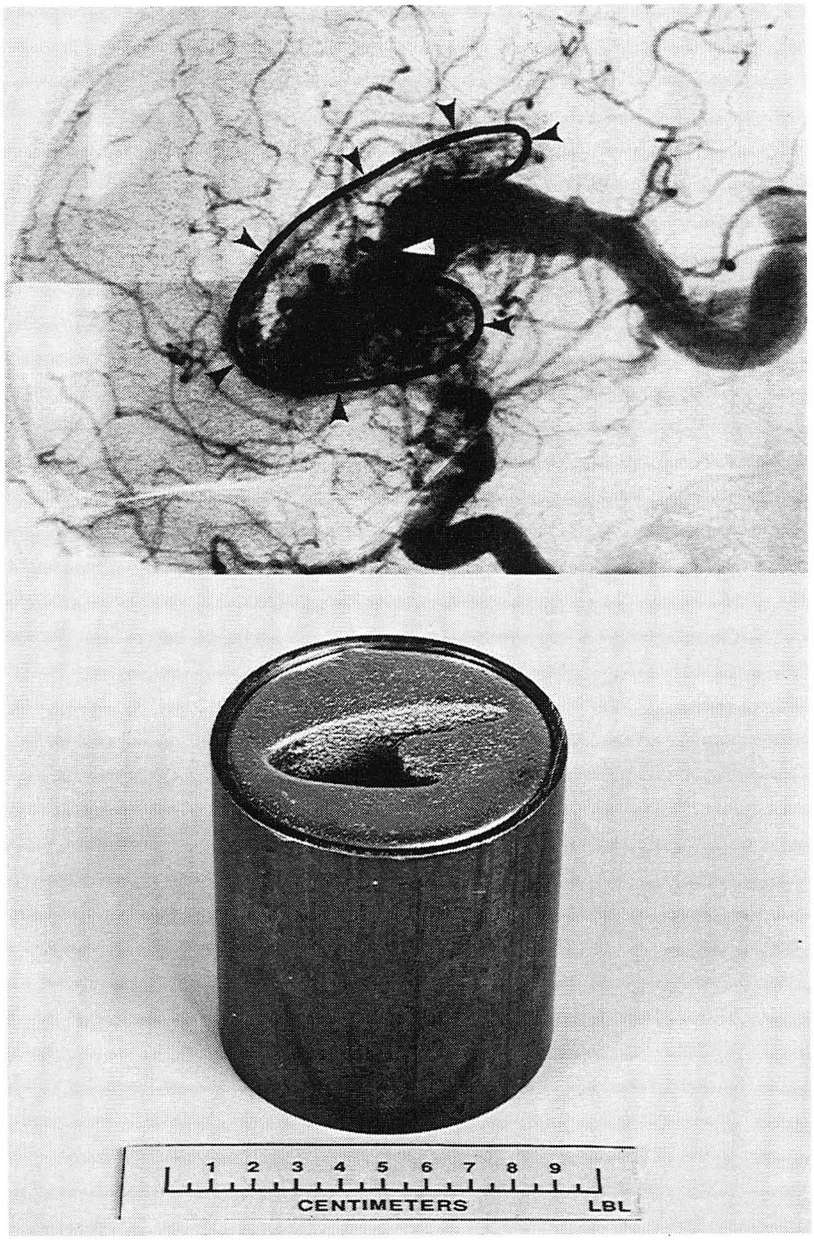

XBB 901-795A

Fig. 3

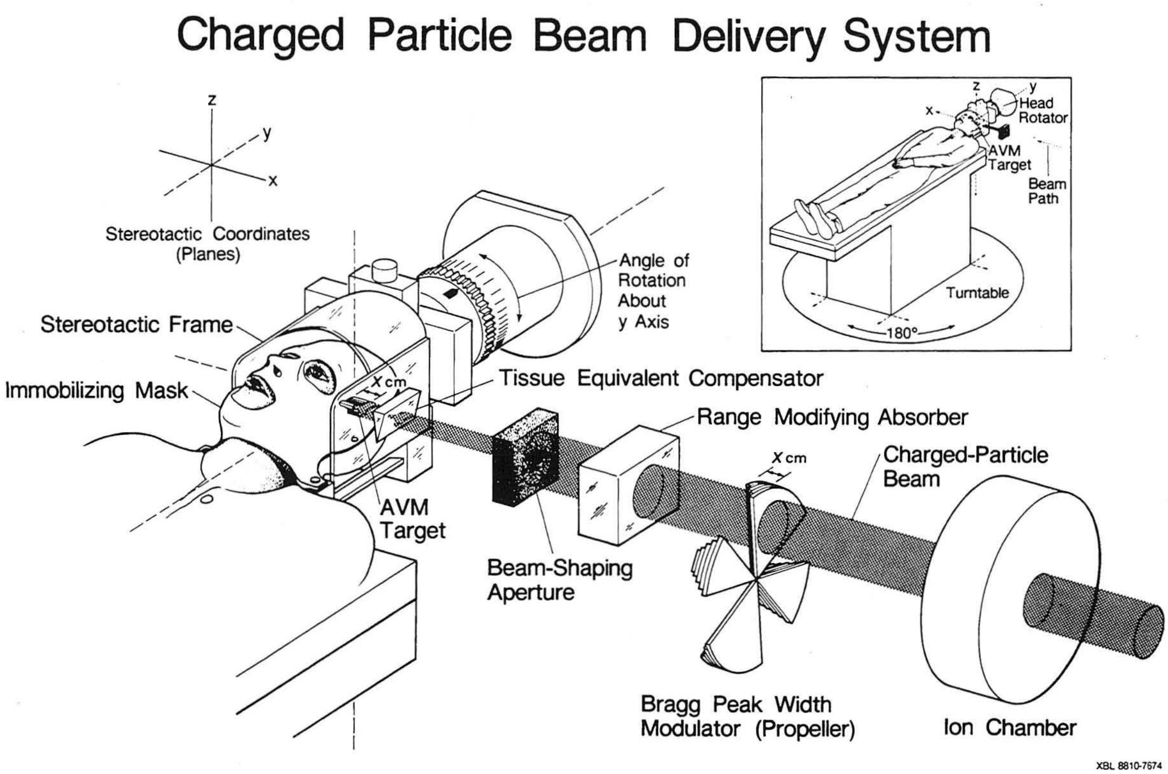
Charged Particle Beam Delivery System
z
y
x
Stereotactic Coordinates (Planes)
Stereotactic Frame
Immobilizing Mask
X cm
AVM Target
Angle of Rotation About y Axis
Tissue Equivalent Compensator
Range Modifying Absorber
X cm
Charged-Particle Beam
Beam-Shaping Aperture
Bragg Peak Width Modulator (Propeller)
Ion Chamber
Head Rotator
AVM Target
Beam Path
Turntable
180°
XBL 8810-7674

Fig. 4

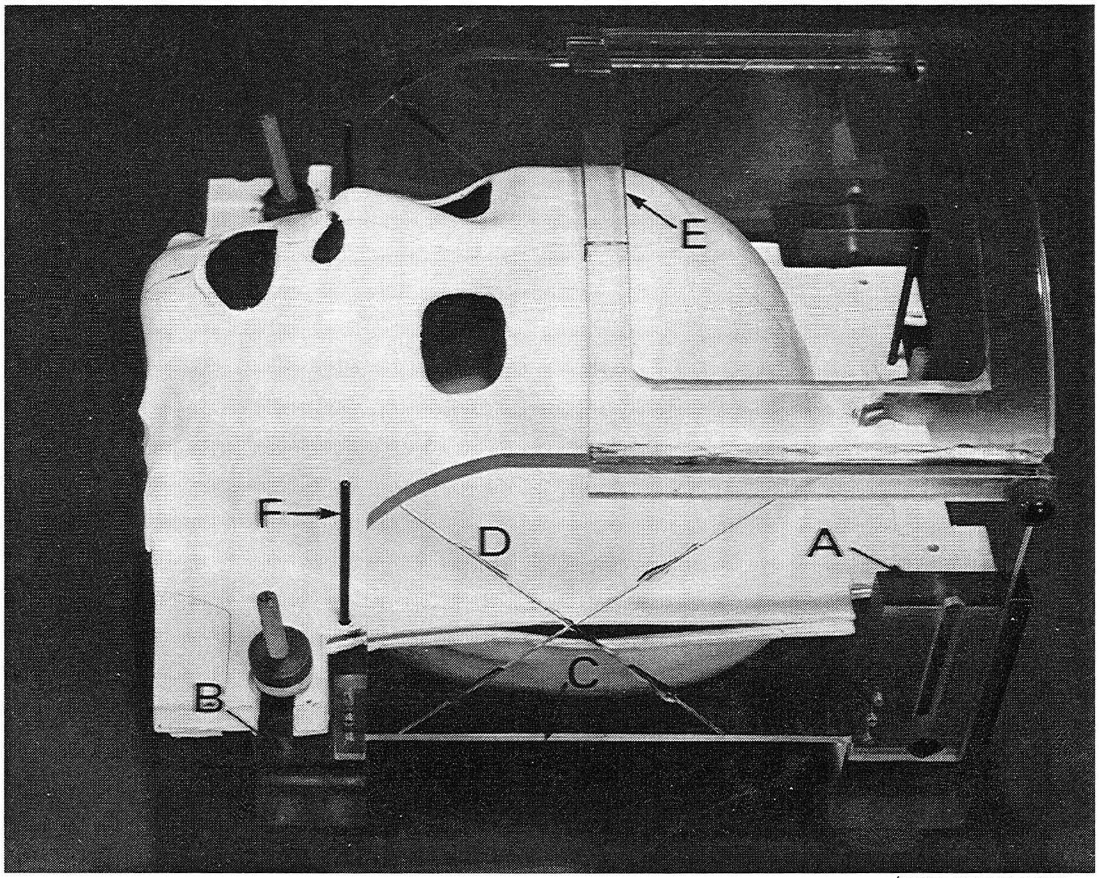

CBB 877-5479A

Fig. 5

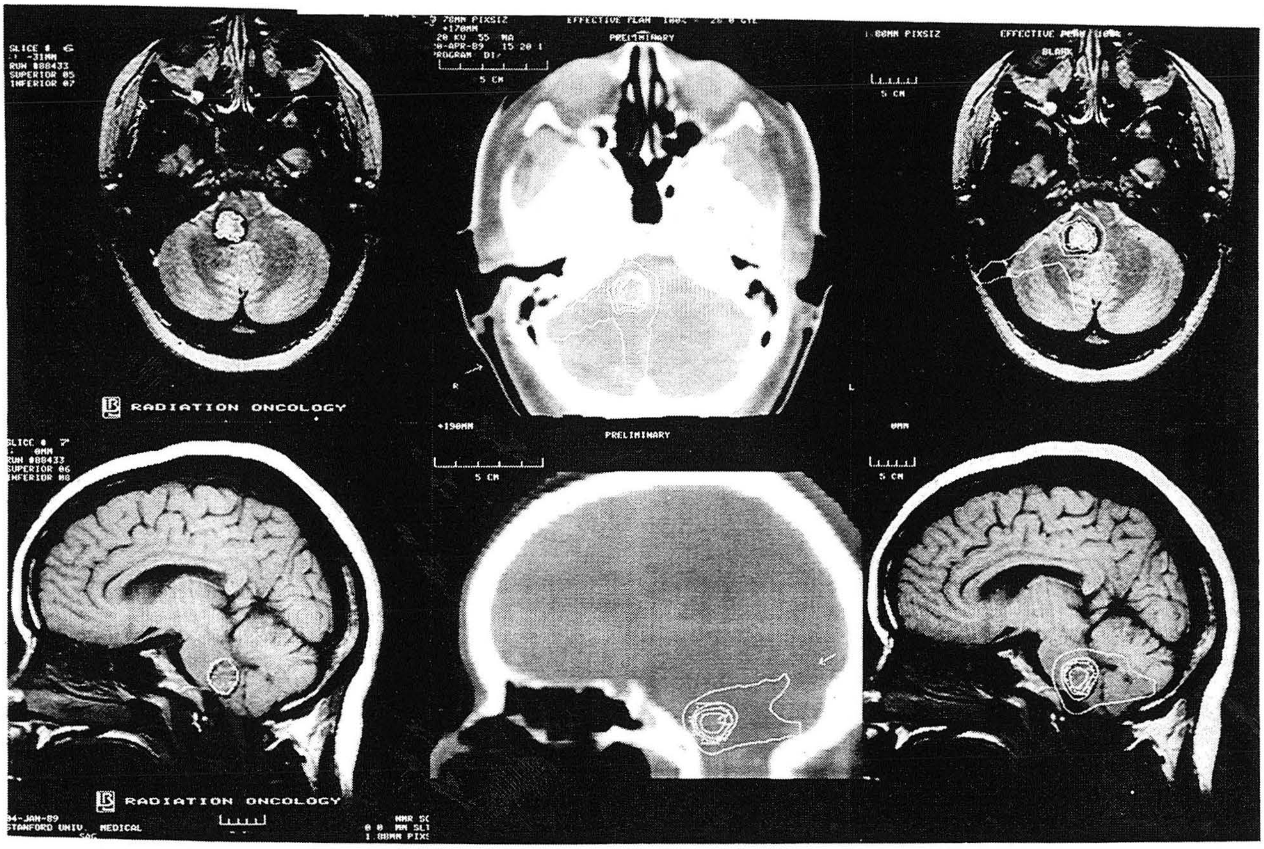

XBB 899-7353

Fig. 6

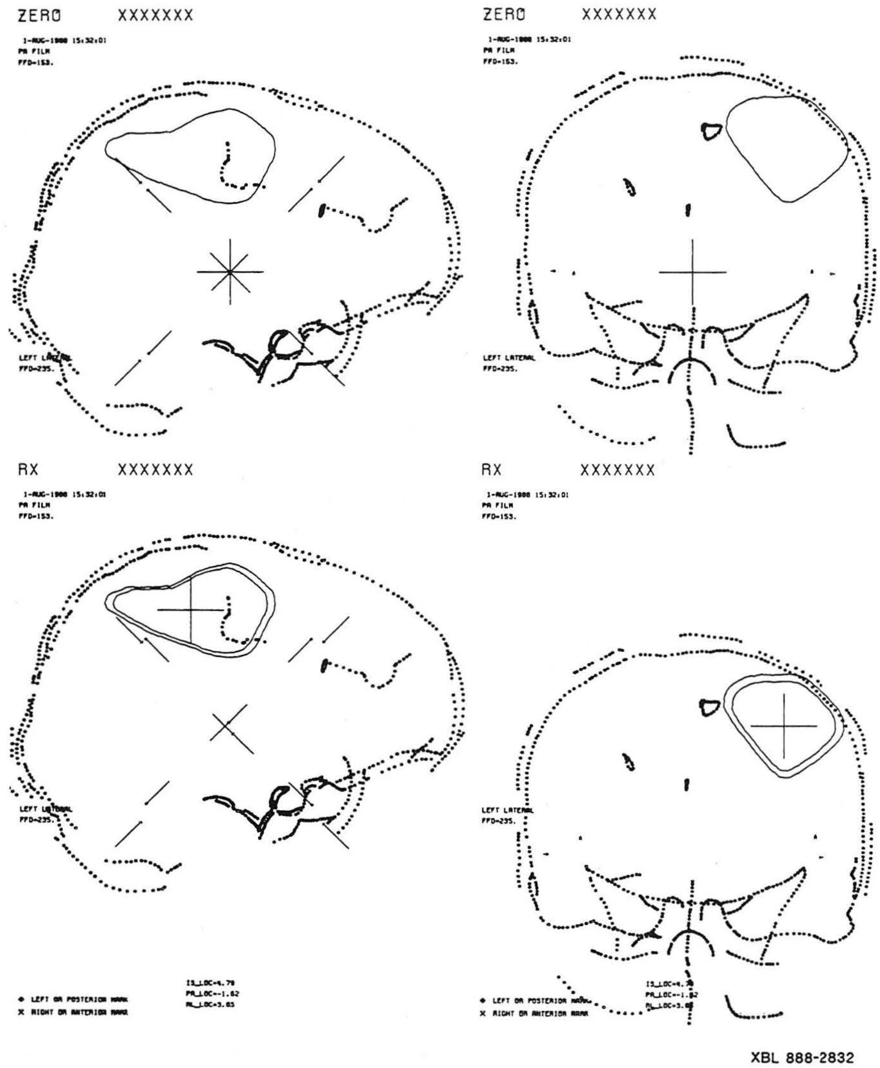
ZERO XXXXXXX
ZERO XXXXXXX
RX XXXXXXX
RX XXXXXXX
XBL 888-2832

Fig. 7

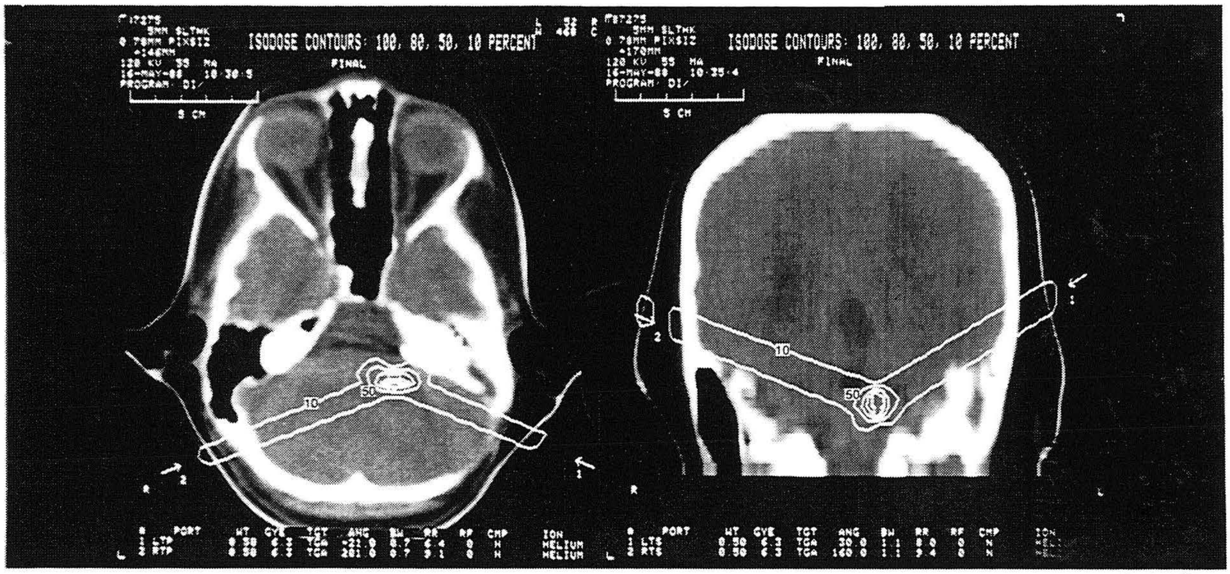

XBB 885-5361A

Fig. 8

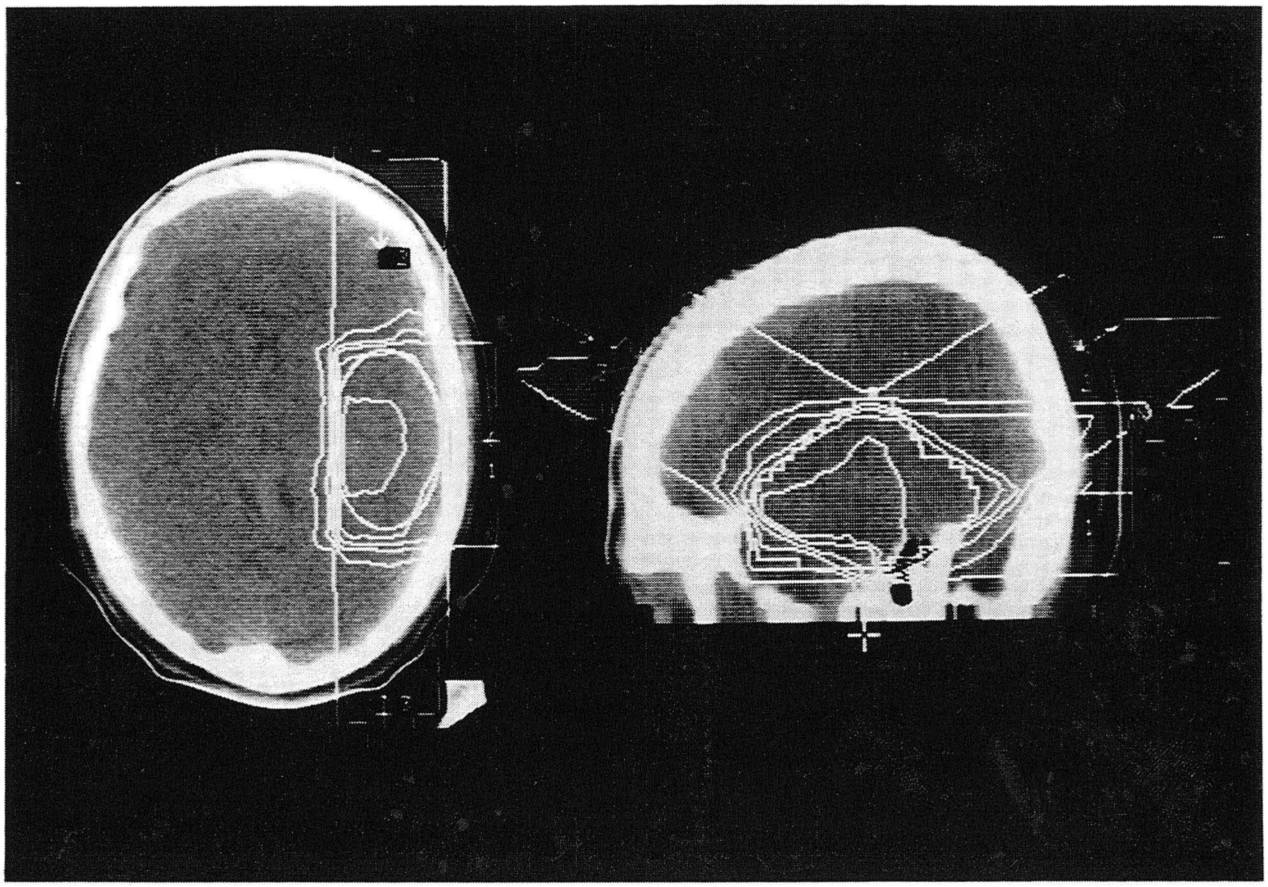

XBB 878-6973A

Fig. 9

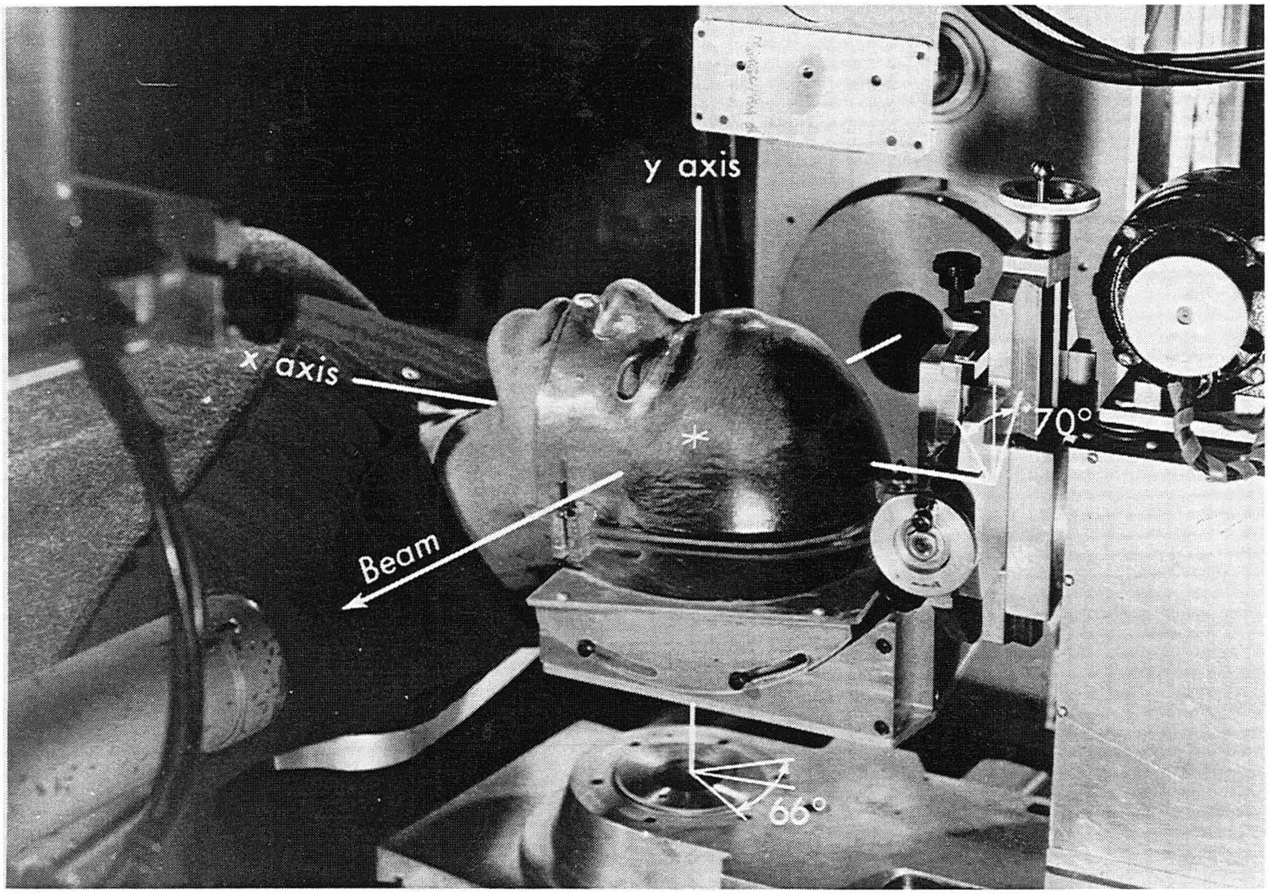

JHL 2897C

Fig. 10

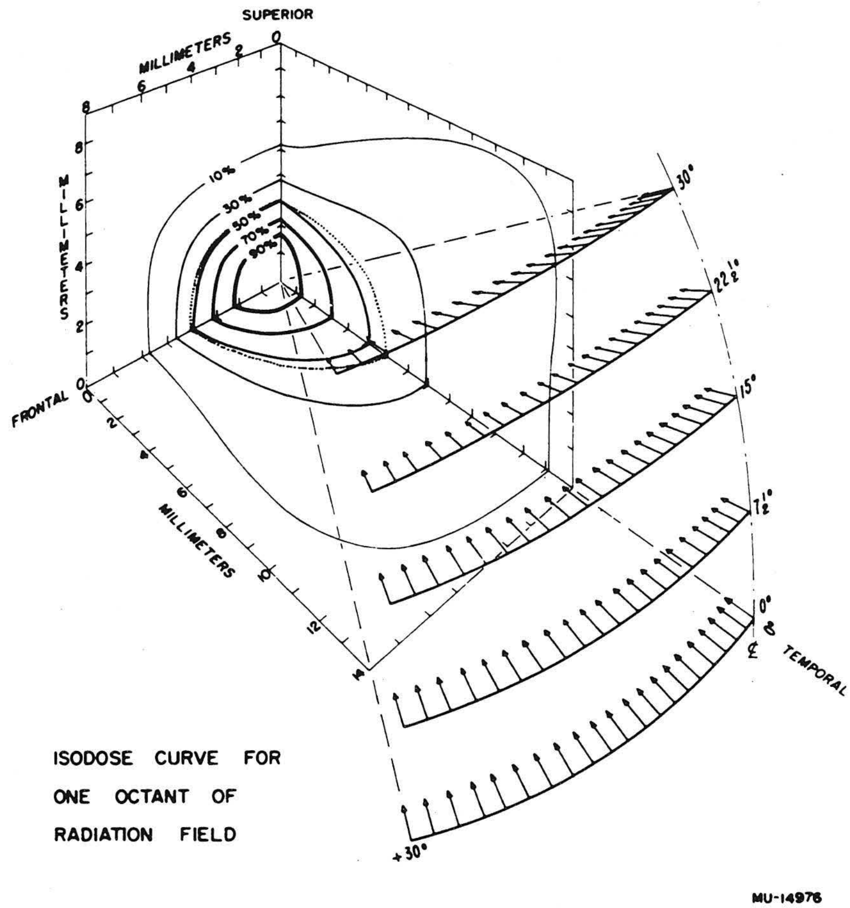
SUPERIOR
MILLIMETERS
FRONTAL
MILLIMETERS
MILLIMETERS
10%
30%
50%
70%
90%
30°
$22\frac{1}{2}°$
15°
$7\frac{1}{2}°$
0°
TEMPORAL
+30°
ISODOSE CURVE FOR
ONE OCTANT OF
RADIATION FIELD
MU-14976

Fig. 11

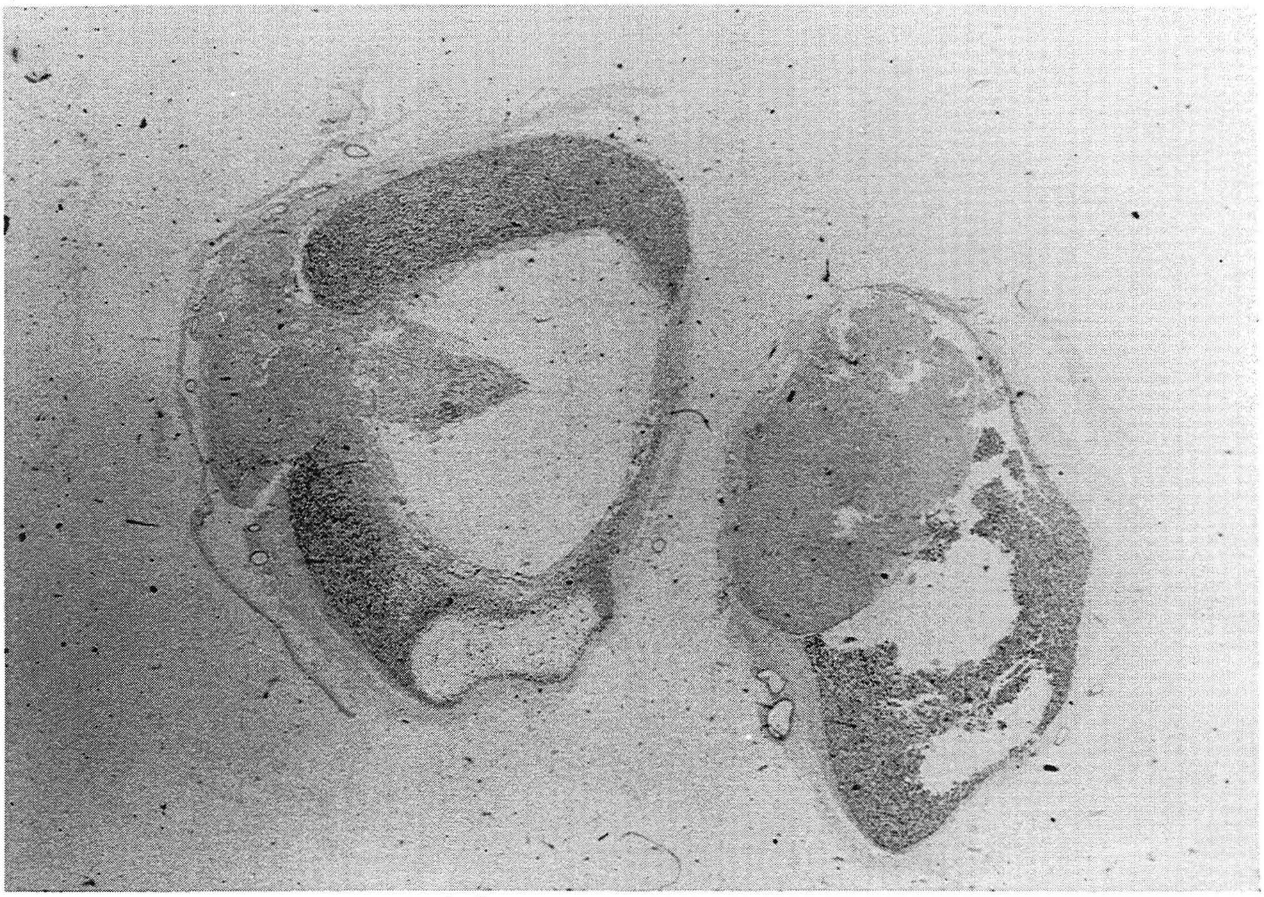

CBB 762-1381

Fig. 12

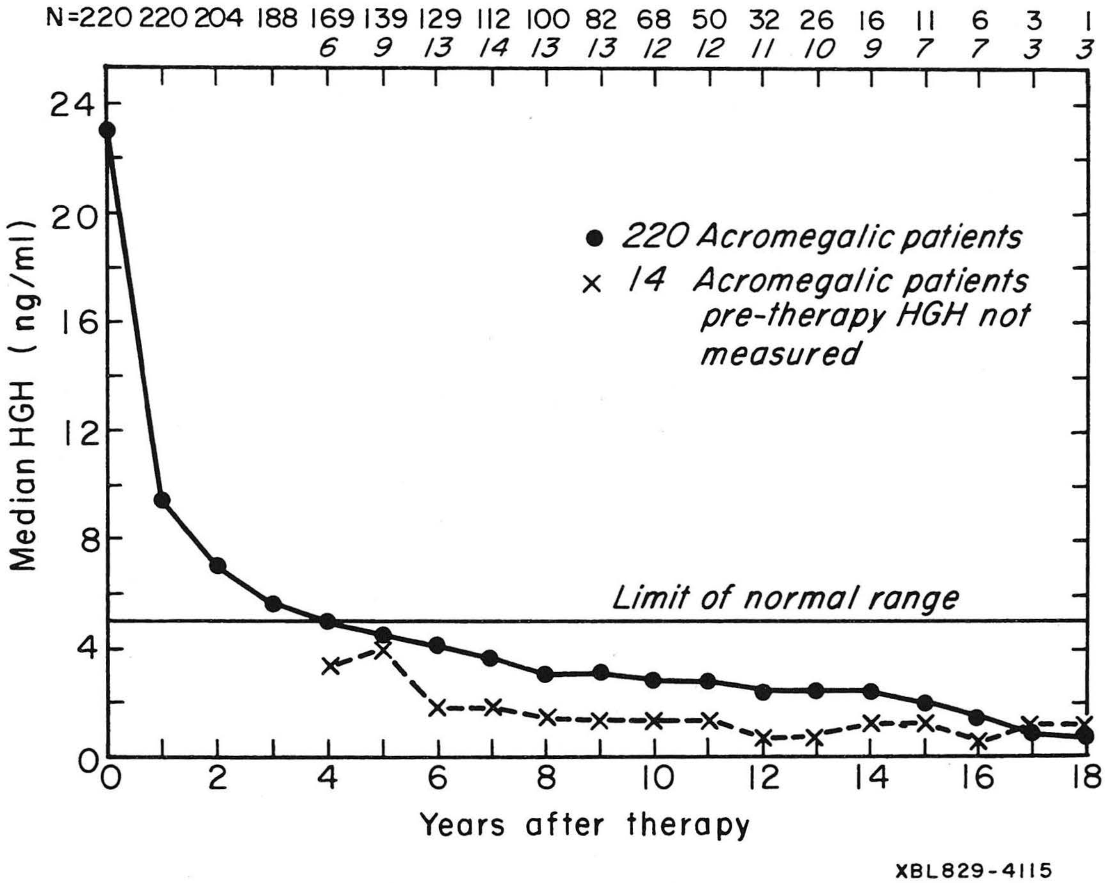
N=220 220 204 188 169 139 129 112 100 82 68 50 32 26 16 11 6 3 1
6 9 13 14 13 13 12 12 11 10 9 7 7 3 3
Median HGH (ng/ml)
0
4
8
12
16
20
24
● 220 Acromegalic patients
× 14 Acromegalic patients pre-therapy HGH not measured
Limit of normal range
0 2 4 6 8 10 12 14 16 18
Years after therapy
XBL829-4115

Fig. 13

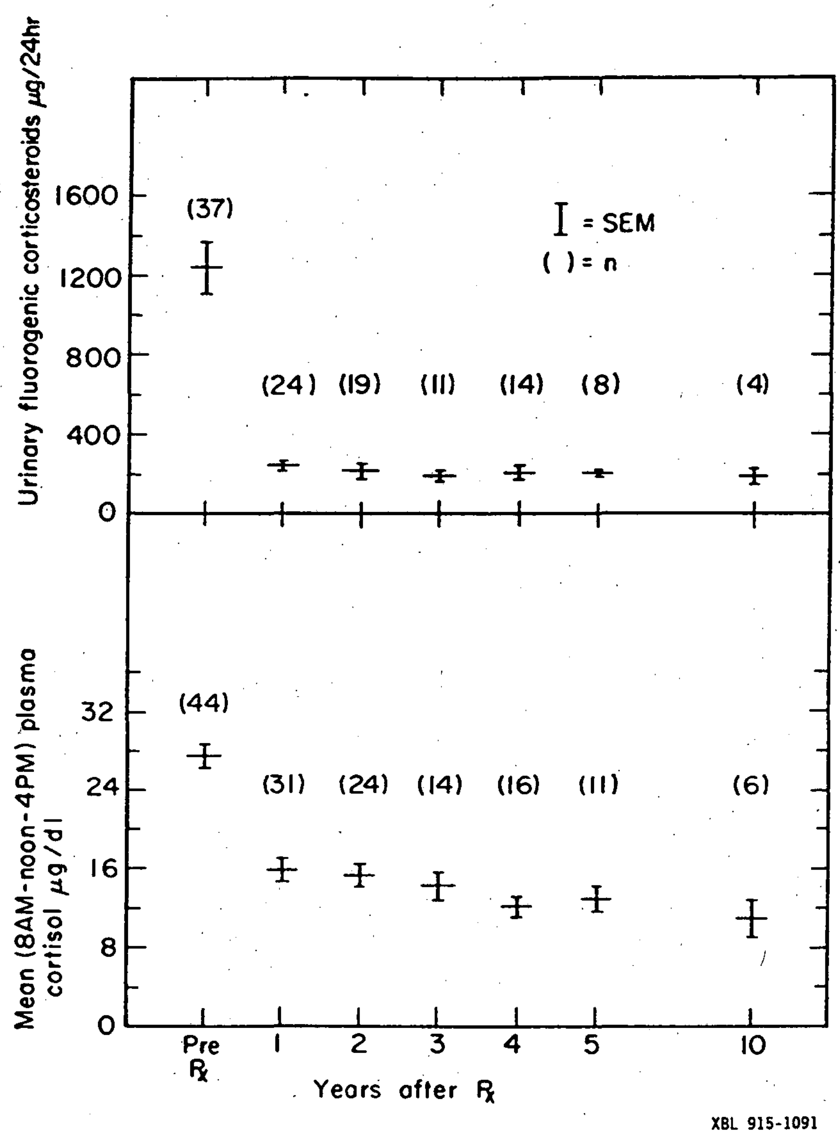
Urinary fluorogenic corticosteroids μg/24hr
1600
1200
800
400
0
(37)
(24)
(19)
(11)
(14)
(8)
(4)
I = SEM
( ) = n
Mean (8AM-noon-4PM) plasma cortisol μg/dl
32
24
16
8
0
(44)
(31)
(24)
(14)
(16)
(11)
(6)
Pre Rx
1
2
3
4
5
10
Years after Rx
XBL 915-1091

Fig. 14

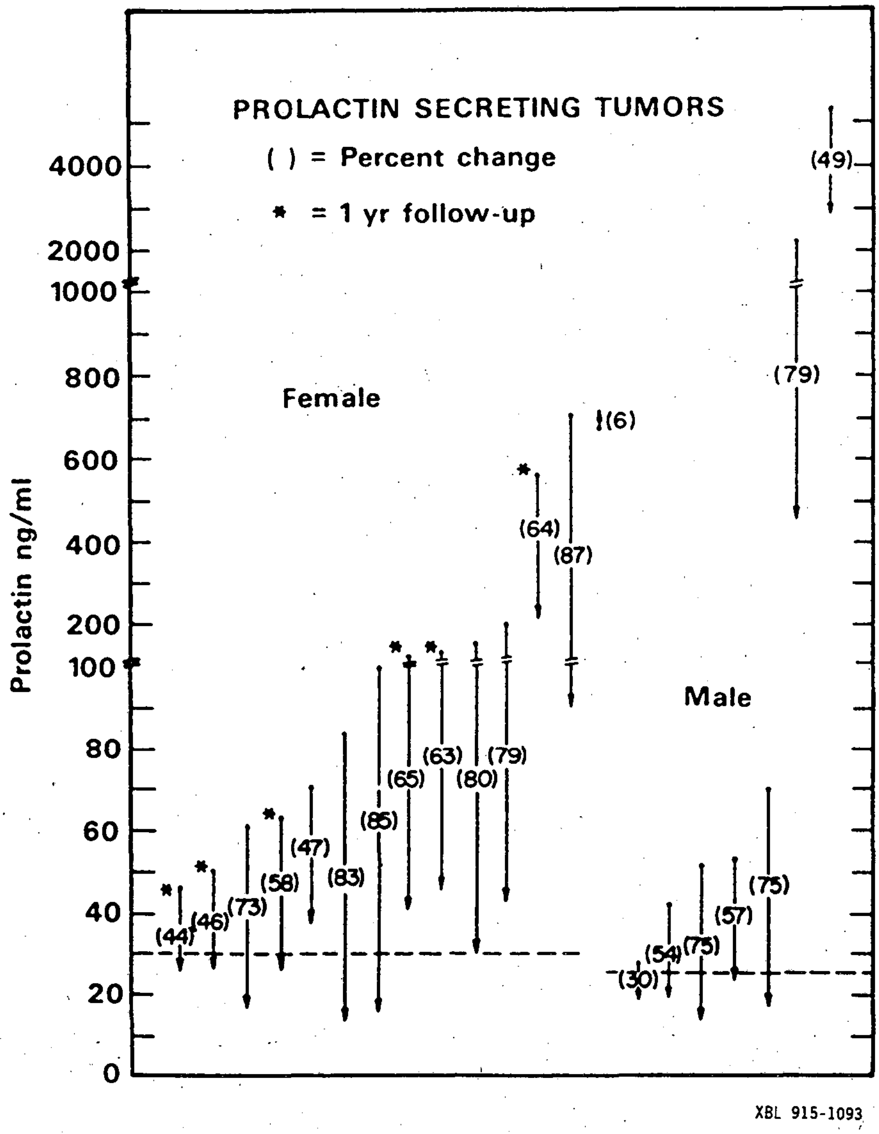
PROLACTIN SECRETING TUMORS
( ) = Percent change
* = 1 yr follow-up
Prolactin ng/ml
4000
2000
1000
800
600
400
200
100
80
60
40
20
0
Female
Male
(44)
(46)
(73)
(58)
(47)
(83)
(85)
(65)
(63)
(80)
(79)
(64)
(87)
(6)
(30)
(54)
(75)
(57)
(75)
(79)
(49)
XBL 915-1093

Fig. 15

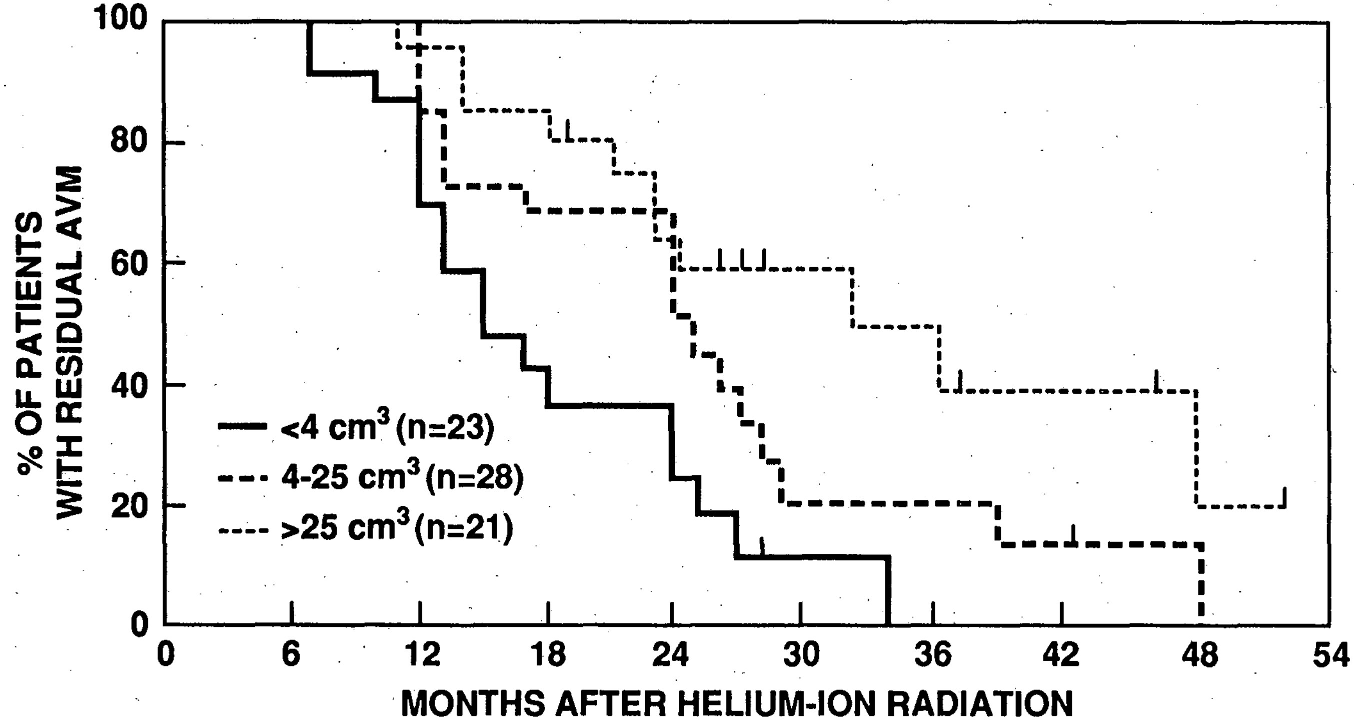
100
80
60
40
20
0
% OF PATIENTS
WITH RESIDUAL AVM
<4 cm3 (n=23)
4-25 cm3 (n=28)
>25 cm3 (n=21)
0
6
12
18
24
30
36
42
48
54
MONTHS AFTER HELIUM-ION RADIATION

Fig. 16

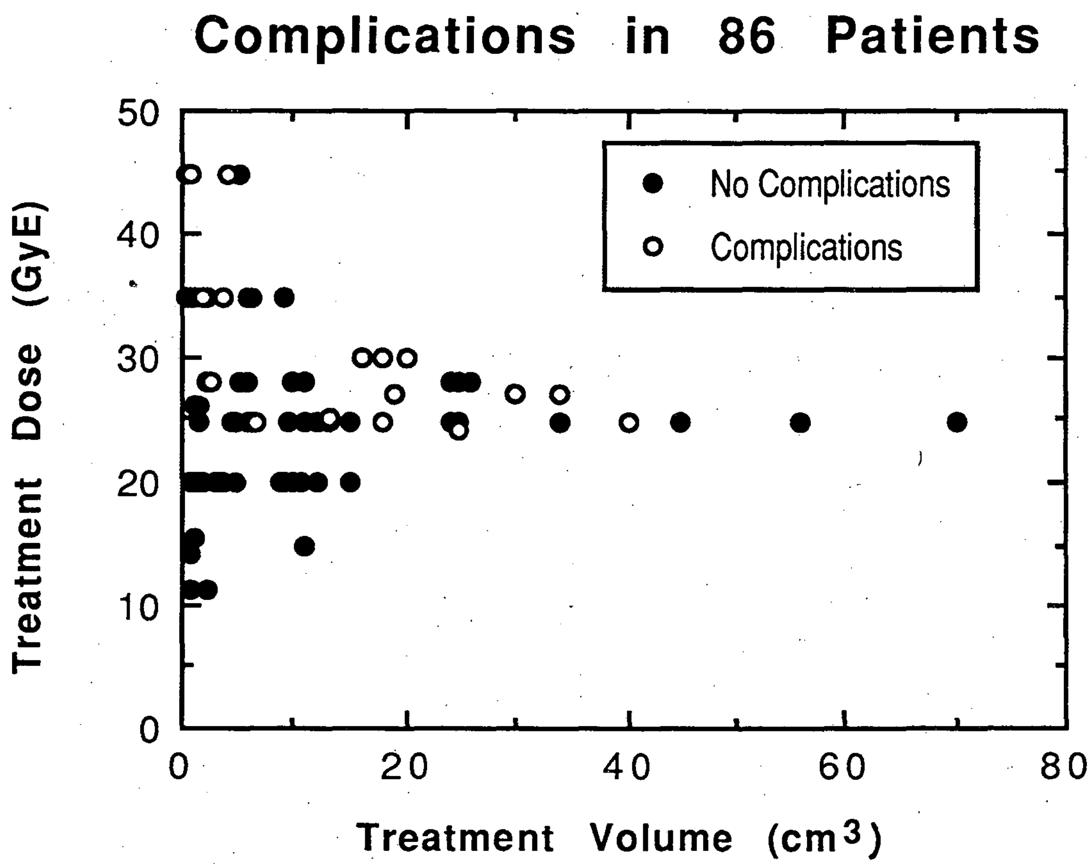
Complications in 86 Patients
Treatment Dose (GyE)
Treatment Volume (cm3)
No Complications
Complications
0
10
20
30
40
50
0
20
40
60
80

Fig. 17